

Transverse structure of the kaon: A light-front Hamiltonian approach

Yuanqi Lu,^{1,2,3,*} Zhimin Zhu,^{1,2,3,†} Jiangshan Lan,^{1,2,3,‡}
Chandan Mondal,^{1,2,3,§} Xingbo Zhao,^{1,2,3,¶} and James P. Vary^{4,**}
(BLFQ Collaboration)

¹*Institute of Modern Physics, Chinese Academy of Sciences, Lanzhou, Gansu, 730000, China*

²*School of Nuclear Physics, University of Chinese Academy of Sciences, Beijing, 100049, China*

³*CAS Key Laboratory of High Precision Nuclear Spectroscopy,*

Institute of Modern Physics, Chinese Academy of Sciences, Lanzhou 730000, China

⁴*Department of Physics and Astronomy, Iowa State University, Ames, IA 50011, USA*

(Dated: March 13, 2026)

We employ the Basis Light-Front Quantization (BLFQ) framework to compute the leading-twist (twist-2) and subleading-twist (twist-3) transverse-momentum-dependent parton distribution functions (TMDs) of the kaon. The light-front wave functions are obtained by diagonalizing a light-front QCD Hamiltonian that includes quark–antiquark ($|q\bar{q}\rangle$) and quark–antiquark–gluon ($|q\bar{q}g\rangle$) Fock components together with a three-dimensional confinement. Using the QCD equations of motion, the twist-3 TMDs are decomposed into twist-2 contributions and genuine twist-3 terms, the latter encoding quark–quark–gluon correlations beyond the probabilistic picture. These genuine twist-3 contributions arise from the interference between the $|q\bar{q}\rangle$ and $|q\bar{q}g\rangle$ sectors, which are usually neglected in the Wandzura–Wilczek approximation. This work provides the first theoretical predictions of kaon subleading-twist TMDs that explicitly account for Fock-sector interference. In addition, we present results for the kaon’s twist-2 and twist-3 collinear parton distribution functions (PDFs). The twist-2 PDFs are found to be in good agreement with the recent global analysis by the JAM Collaboration.

I. INTRODUCTION

Understanding the internal structure of hadrons is a central goal of modern particle and nuclear physics [1–6]. Direct access to this structure from the QCD first principles remains difficult due to the unresolved challenges of color confinement and chiral symmetry breaking. Nevertheless, the development of QCD factorization theorems [6–14] allows one to separate experimental cross sections into short-distance perturbative contributions and long-distance nonperturbative components, with the latter encoding hadron structure [13, 15–18]. A prime example is the extraction of collinear parton distribution functions (PDFs) from deep inelastic scattering (DIS) data [19, 20]. PDFs describe the distribution of the longitudinal momentum fraction carried by hadronic constituents [7, 21], thereby providing a one-dimensional view of hadron structure.

Beyond the one-dimensional description offered by PDFs, the three-dimensional (3D) structure of hadrons can be explored through generalized parton distributions (GPDs) [6, 22–25] and transverse-momentum-dependent parton distribution functions (TMDs) [26–29]. GPDs provide access to the spatial distribution and orbital motion of partons inside hadrons [6, 30–32], and can be extracted experimentally from exclusive processes such as

deeply virtual Compton scattering (DVCS) and deeply virtual meson production (DVMP) [6, 25, 33–35]. TMDs, in contrast, encode information about the transverse momentum distribution of partons in addition to their longitudinal momentum fraction [7]. They can be extracted, particularly for quarks, from azimuthal-angle-dependent cross sections in semi-inclusive deep inelastic scattering (SIDIS) and Drell–Yan processes [7, 36–38]. Together, GPDs and TMDs provide complementary insights that enable a three-dimensional tomography of hadrons.

In theoretical descriptions of high-energy scattering processes, cross sections are expanded in powers of $1/Q$, where Q is the scattering energy scale [39]. The leading term in this expansion is governed by leading-twist (twist-2) distributions, which in the parton model are interpreted as probability densities for finding partons inside a hadron [7, 21, 40, 41]. Subleading contributions arise at twist-3, where the distributions go beyond the simple probabilistic picture and encode multiparton correlations within the hadron [42–45].

The main purpose of this work is to systematically explore the subleading-twist (twist-3) TMDs of the kaon, going beyond the Wandzura–Wilczek (WW) approximation [2, 46–48]. Twist-3 TMDs are not independent quantities; rather, through the QCD equations of motion, they can be decomposed into contributions from twist-2 distributions and genuine twist-3 terms [40, 47, 49]. The latter encode quark–quark–gluon correlations and arise from the interference between different light-front Fock sectors, specifically $|q\bar{q}\rangle$ and $|q\bar{q}g\rangle$, which are typically neglected within the WW approximation. We compute the kaon TMDs using its light-front wave functions (LFWFs) obtained by diagonalizing the light-front QCD

* yuanqilu@impcas.ac.cn

† zhuzhimin@impcas.ac.cn

‡ jiangshanlan@impcas.ac.cn

§ mondal@impcas.ac.cn

¶ xbzhao@impcas.ac.cn

** jvary@iastate.edu

Hamiltonian. Our results provide new nonperturbative input on higher-twist dynamics, particularly the role of multi-parton interference, which will be relevant for future experimental studies at facilities such as the upcoming Electron–Ion Colliders in China (EicC) and the USA (EIC).

Twist-3 PDFs and TMDs contribute to a variety of observables in inclusive and semi-inclusive deep inelastic scattering (DIS and SIDIS). Although typically suppressed relative to twist-2, twist-3 effects can be significant in fixed-target kinematics. Indeed, one of the main goals of the Jefferson Lab 12 GeV program is to measure higher-twist spin-dependent azimuthal asymmetries in SIDIS [50–52], while the upcoming EICs [45, 53–55] will extend such studies to new kinematic regions [1, 56].

To date, twist-3 TMDs have been investigated within a variety of QCD-inspired models and perturbative light-front Hamiltonian approaches [43, 57–77]. More recently, unpolarized twist-2 and twist-3 time-reversal-even quark TMDs of the pion have been computed using the homogeneous Bethe–Salpeter integral equation [78] and the Basis Light-Front Quantization (BLFQ) framework [79], while phenomenological extractions from pion–nucleus Drell–Yan data have been reported in Refs. [80, 81].

Although the kaon has received less attention than the pion, it represents an equally important probe of the underlying dynamics of the Standard Model. Kaons provide a rich source of information on the nature of fundamental interactions, including insights into the quark model of hadrons [82]. Moreover, studies of kaon structure and dynamics serve as a valuable tool for exploring electroweak interactions and for advancing our understanding of CP violation [83–85]. In this context, investigating the partonic structure of the kaon through TMDs offers a unique opportunity to uncover its three-dimensional dynamics and to complement existing studies of the pion.

In this work, we present the twist-2 and twist-3 TMDs of the kaon obtained within the BLFQ framework [86, 87], which is a nonperturbative approach for solving relativistic many-body bound-state problems in quantum field theory [32, 86–104]. This framework has previously been applied successfully to study the leading-twist TMDs of spin- $\frac{1}{2}$ and spin-1 particles in QED, such as the electron [99] and the photon [95], as well as for the proton [105]. More recently, the BLFQ framework has been extended to successfully investigate subleading twist TMDs of the pion [79] and the TMDs and GPDs of the proton [106–108].

We stress that our computation of kaon TMDs is performed at the model scale, without incorporating the effects of TMD evolution [7, 109–112]. Within the nonperturbative BLFQ framework, the results should therefore be interpreted as representing the intrinsic, initial-scale structure of the kaon. In this sense, our calculation provides a physically motivated starting point for the kaon TMDs, while the inclusion of TMD evolution would be necessary to make direct comparisons with experimental data at higher scales. Such an analysis, however, lies

beyond the scope of the present work.

Within the BLFQ framework [86], we employ the light-front QCD Hamiltonian [96, 113] and solve for its mass eigenvalues and eigenstates. The Hamiltonian is constructed with quark (q), antiquark (\bar{q}), and gluon (g) degrees of freedom, incorporating light-front QCD interactions relevant to the constituent $|q\bar{q}\rangle$ and $|q\bar{q}g\rangle$ Fock sectors of mesons, together with a complementary three-dimensional confinement potential [89]. We solve this Hamiltonian in the leading two Fock sectors and determine the model parameters by fitting the mass spectra of light mesons, including the kaon [96]. The resulting LFWFs, obtained as Hamiltonian eigenstates, have already been successfully applied to describe a wide range of kaon observables, such as electromagnetic form factors, charge radius, decay constant, PDFs, and even cross sections for kaon-induced charmonium production, revealing consistency with available experimental measurements and other models [90, 114, 115]. In this work, we extend these studies to compute the kaon’s subleading-twist TMDs and, for the first time, to predict the genuine twist-3 TMDs. In addition, we present results for the kaon’s twist-2 and twist-3 collinear PDFs. The twist-2 PDFs are found to be in good agreement with the recent global analysis by the JAM Collaboration [116].

II. BASIS LIGHT-FRONT QUANTIZATION FRAMEWORK

In light-front field theory, bound states are obtained by solving the light-front stationary Schrödinger equation,

$$P^+ P^- |\Psi\rangle = M^2 |\Psi\rangle, \quad (1)$$

where $P^- = P^0 - P^3$ is the light-front Hamiltonian, $P^+ = P^0 + P^3$ is the longitudinal momentum of the system, and M^2 is the invariant mass squared of the state. At fixed light-front time, $x^+ \equiv x^0 + x^3$, the meson state can be expanded in terms of its quark, antiquark, and gluon Fock components,

$$|\Psi\rangle = \psi_{(q\bar{q})} |q\bar{q}\rangle + \psi_{(q\bar{q}g)} |q\bar{q}g\rangle + \psi_{(q\bar{q}q\bar{q})} |q\bar{q}q\bar{q}\rangle + \dots, \quad (2)$$

where $\psi_{(\dots)}$ denotes the LFWF corresponding to a given Fock sector. For practical calculations, this infinite expansion must be truncated. In the present work, we retain only the lowest two sectors, namely the quark–antiquark ($\psi_{(q\bar{q})}$) and quark–antiquark–gluon ($\psi_{(q\bar{q}g)}$) components, which characterize the meson structure at the model scale.

To address the eigenvalue problem, we introduce an effective light-front Hamiltonian of the form $P^- = P_{\text{QCD}}^- + P_{\text{C}}^-$, where P_{QCD}^- represents the light-front QCD Hamiltonian describing the dynamics of the quark–antiquark ($|q\bar{q}\rangle$) and quark–antiquark–gluon ($|q\bar{q}g\rangle$) Fock sectors, while P_{C}^- denotes the model Hamiltonian implementing the confining interaction [96].

In the light-front gauge $A^+ = 0$, the explicit form of the QCD Hamiltonian with a single dynamical gluon reads [79, 117, 118]:

$$P_{\text{QCD}}^- = \int dx^- d^2x^\perp \left\{ \frac{1}{2} \bar{\psi} \gamma^+ \frac{m_0^2 + (i\partial^\perp)^2}{i\partial^+} \psi \right. \\ \left. + \frac{1}{2} A_a^i [m_g^2 + (i\partial^\perp)^2] A_a^i + g \bar{\psi} \gamma_\mu T^a A_a^\mu \psi \right. \\ \left. + \frac{1}{2} g^2 \bar{\psi} \gamma^+ T^a \psi \frac{1}{(i\partial^+)^2} \bar{\psi} \gamma^+ T^a \psi \right\}, \quad (3)$$

where ψ and A^μ denote the quark and gluon fields, respectively, with $T^a = \lambda^a/2$ the SU(3) color generators. $\gamma^+ = \gamma^0 + \gamma^3$, represents the plus component of the Dirac matrices in light-front coordinates. The parameter g is the QCD coupling constant, while m_0 and m_g represent the bare quark mass and the model gluon mass, respectively. Although gluons are massless in QCD, a phenomenologically motivated gluon mass is introduced in our low-energy model to reproduce the meson mass spectra [96]. To account for quark mass corrections from higher Fock sectors, we include a mass counterterm $\delta m_q = m_0 - m_q$ in the leading Fock sector, where m_q is the renormalized quark mass. In addition, an independent quark mass m_f is used in the vertex interaction, following Refs. [119, 120].

The confining interaction in the leading $|q\bar{q}\rangle$ Fock sector consists of transverse and longitudinal contributions [89, 96],

$$P_C^- P^+ = \kappa^4 \left\{ x(1-x) \bar{r}_\perp^2 - \frac{\partial_x [x(1-x) \partial_x]}{(m_q + m_{\bar{q}})^2} \right\}, \quad (4)$$

where κ denotes the confinement strength and $\bar{r}_\perp = \sqrt{x(1-x)}(\bar{r}_{\perp q} - \bar{r}_{\perp \bar{q}})$ is the holographic variable [121]. In the $|q\bar{q}g\rangle$ sector, confinement is implemented through the introduction of a massive gluon together with a truncation of the BLFQ basis functions, as described below.

We employ the BLFQ framework [86–89, 94, 96, 122–124], a nonperturbative approach for solving the light-front eigenvalue problem, Eq. (1). Each Fock sector $|\dots\rangle$ in Eq. (2) is constructed as a direct product of single-particle states $|\alpha\rangle = \otimes_i |\alpha_i\rangle$.

In BLFQ, the longitudinal degrees of freedom are represented using the Discretized Light-Cone Quantization (DLCQ) basis [113]. A fermion (boson) is confined to a one-dimensional box of length $2L$ with antiperiodic (periodic) boundary conditions, leading to longitudinal momenta

$$p^+ = \frac{2\pi}{L} k, \quad (5)$$

where k is a half-integer for fermions and an integer for bosons. Zero modes for bosons are neglected.

The transverse degrees of freedom are described by two-dimensional harmonic-oscillator (2D-HO) basis functions $\Phi_{nm}(p_\perp, b)$, with oscillator scale b . Here, n and m denote the radial and angular quantum numbers, respectively.

Each single-particle basis state is specified by four quantum numbers, $|\alpha_i\rangle = |k_i, n_i, m_i, \lambda_i\rangle$, where λ_i denotes the light-front helicity. For Fock sectors that allow multiple color-singlet states (beyond those considered here), an additional label is required to distinguish among them.

Finally, the many-body basis states constructed in BLFQ have well-defined total angular momentum projection,

$$M_J = \sum_i (m_i + \lambda_i). \quad (6)$$

For numerical calculations, the infinite basis of each Fock sector is truncated by introducing two truncation parameters K and N_{max} in longitudinal and transverse directions, respectively. The parameter $K = \sum_i k_i$ limits the total longitudinal momentum quantum numbers. Hence, for every parton indexed by i , the longitudinal momentum fraction is given by $x_i = p_i^+/P^+ = k_i/K$. In the transverse direction, the parameter N_{max} , set by $\sum_i (2n_i + |m_i| + 1) \leq N_{\text{max}}$, characterizes the truncation of the transverse center of mass motion [87, 88]. The N_{max} truncation implicitly sets the infrared (IR) and ultraviolet (UV) cutoffs in momentum space: the IR cutoff $\lambda_{\text{IR}} \simeq b/\sqrt{N_{\text{max}}}$ and the UV cutoff $\Lambda_{\text{UV}} \simeq b\sqrt{N_{\text{max}}}$ [87].

By diagonalizing the Hamiltonian matrix, we obtain the mass spectra M^2 and the corresponding LFWFs. The LFWF in the momentum space is schematically represented as

$$\Psi_{\mathcal{N}, \{\lambda_i\}}^{M_J}(\{x_i, p_{\perp i}\}) = \sum_{\{n_i, m_i\}} \psi_{\mathcal{N}}^{M_J}(\{\alpha_i\}) \prod_{i=1}^{\mathcal{N}} \Phi_{n_i, m_i}(p_{\perp i}, b), \quad (7)$$

where $\psi_{\mathcal{N}=2}^{M_J}(\{\alpha_i\})$ and $\psi_{\mathcal{N}=3}^{M_J}(\{\alpha_i\})$ represent the eigenvector components corresponding to the $|q\bar{q}\rangle$ and $|q\bar{q}g\rangle$ Fock sectors, respectively. Using the truncation parameters $\{N_{\text{max}}, K\} = \{14, 15\}$, the model parameters listed in Table I were determined to reproduce the mass spectra of strange mesons [82]. The resulting LFWFs provide a good quality description of a wide range of observables, including the kaon's electromagnetic form factor and charge radius, decay constant, PDFs, as well as the kaon-nucleus-induced Drell-Yan cross section, which is expected to be measured soon by COMPASS++/AMBER at CERN [82].

TABLE I. Model parameters $m_q, m_{f_q}, m_g, b, \kappa, g$ are taken from Ref. [96], while the strange quark masses m_s and m_{f_s} are fixed by fitting the experimental masses of $\phi(1020)$ and $f_1(1420)$ [82]. All values are in units of GeV, except for the coupling g .

| m_q | m_{f_q} | m_g | b | κ | g | m_s | m_{f_s} |
|-------|-----------|-------|------|----------|------|-------|-----------|
| 0.39 | 5.69 | 0.60 | 0.29 | 0.65 | 1.92 | 0.55 | 7.13 |

III. TRANSVERSE-MOMENTUM-DEPENDENT PARTON DISTRIBUTIONS

In the light-front formalism, quark and gluon TMDs are defined through the quark–quark and unintegrated gluon correlation functions, respectively [125–127]:

$$\Phi_q^{[\Gamma]}(x, k_\perp) = \frac{1}{2} \int \frac{dz^- d^2 \vec{z}_\perp}{2(2\pi)^3} e^{ik \cdot z} \times \langle P | \bar{\psi}(0) \Gamma \mathcal{W}(0, z) \psi(z) | P \rangle |_{z^+=0}, \quad (8)$$

$$\Phi^{g[ij]}(x, k_\perp) = \frac{1}{xP^+} \int \frac{dz^- d^2 z_\perp}{2(2\pi)^2} e^{ik \cdot z} \times \langle P | F^{+j}(0) \mathcal{W}(0, z) F^{+i}(z) | P \rangle |_{z^+=0}, \quad (9)$$

where $F^{\mu\nu}$ is the gluon field strength tensor. Here, $|P\rangle$ denotes the light-front bound state of the target meson with mass M and momenta (P^+, P_\perp) , where we choose $P_\perp = 0$ [128]. The Dirac matrix Γ specifies the Lorentz structure of the correlator $\Phi^{[\Gamma]}$ and determines its twist- τ [42]. The Wilson line \mathcal{W} ensures gauge invariance of the bilocal quark field operators in the correlation function [129].

For spin-0 mesons, two leading-twist (twist-2) quark TMDs appear: the unpolarized distribution $f_1^q(x, k_\perp)$ and the Boer–Mulders function $h_1^{\perp q}(x, k_\perp)$. These are obtained from the parameterization of the quark–quark correlator with $\Gamma \equiv \gamma^+$ and $\Gamma \equiv \sigma^{j+} \gamma_5$, respectively [130, 131]:

$$\Phi_q^{[\gamma^+]}(x, k_\perp) = f_1^q(x, k_\perp), \quad (10)$$

$$\Phi_q^{[i\sigma^{j+}\gamma_5]}(x, k_\perp) = -\frac{\varepsilon_T^{ij} k_\perp^i}{M} h_1^{\perp q}(x, k_\perp). \quad (11)$$

where k_\perp is the transverse momentum of a struck parton, ε_T^{ij} is an antisymmetric tensor, $\varepsilon_T^{11} = \varepsilon_T^{22} = 0$ and $\varepsilon_T^{12} = -\varepsilon_T^{21} = 1$. Meanwhile, the unpolarized twist-2 gluon TMDs are defined through the correlator as [132]

$$\Phi^g(x, k_\perp) = \delta^{ij} \Phi^{g[ij]}(x, k_\perp) = f_1^g(x, k_\perp). \quad (12)$$

The subleading twist (twist-3) quark TMDs are defined as follows [125]:

$$\Phi_q^{[1]}(x, k_\perp) = \frac{M}{P^+} e^q(x, k_\perp), \quad (13)$$

$$\Phi_q^{[\gamma^j]}(x, k_\perp) = \frac{M}{P^+} \frac{k_\perp^j}{M} f^{\perp q}(x, k_\perp), \quad (14)$$

$$\Phi_q^{[i\gamma_5]}(x, k_\perp) = -\frac{M}{P^+} \frac{\varepsilon_T^{ij} k_\perp^i}{M} g^{\perp q}(x, k_\perp), \quad (15)$$

$$\Phi_q^{[i\varepsilon^{ij}\gamma_5]}(x, k_\perp) = -\frac{M}{P^+} \varepsilon_T^{ij} h^q(x, k_\perp). \quad (16)$$

Note that the TMDs $h_1^{\perp q}(x, k_\perp)$, $g^{\perp q}(x, k_\perp)$, and $h^q(x, k_\perp)$ are time-reversal-odd (T-odd), while all others are time-reversal-even (T-even) [133]. Twist-3 TMD correlation functions are further suppressed by a factor of M/P^+ . In the present work, we neglect the nontrivial

effect of the Wilson line \mathcal{W} by approximating it as the identity operator, $\mathcal{W} \approx 1$. Under this approximation, only the T-even TMDs remain [71].

We decompose the quark field ψ into a “good” component ψ_+ and a “bad” component ψ_- , defined as $\psi_\pm = \frac{1}{4} \gamma^\mp \gamma^\pm \psi$ in light-front field theory [134]. The bad component ψ_- can be represented by ψ_+ and the gauge fields as

$$\psi_-(z) = \frac{\gamma^+}{2i\partial^+} [i(\partial_j - igA_{\perp j}(z))\gamma_j + m_q] \psi_+(z). \quad (17)$$

Note that m_q describes the quark mass and $j = 1, 2$. This constraint equation follows from the equations of motion in the light-cone gauge, $A^+ = 0$ [118].

At leading twist, Eq. (10), the relevant Dirac matrices project the correlator onto $\bar{\psi}_+ \psi_+$. In contrast, for subleading twist, Eq. (13), the Dirac structures project onto $\bar{\psi}_+ \psi_- + \bar{\psi}_- \psi_+$. Consequently, twist-3 TMDs cannot be interpreted as probability densities (or their differences); instead, they are expressed in terms of quark–quark and quark–quark–gluon matrix elements.

Following the EOM of quark fields [135], the higher-twist operators can be decomposed into a combination of twist-2 and genuine higher-twist contributions. Accordingly, the twist-2 and the twist-3 TMDs are related through the following relations [79, 136]:

$$xe^q(x, k_\perp) = x\tilde{e}^q(x, k_\perp) + \frac{m_q}{M} f_1^q(x, k_\perp), \quad (18)$$

$$xf^{\perp q}(x, k_\perp) = x\tilde{f}^{\perp q}(x, k_\perp) + f_1^q(x, k_\perp),$$

where the tilde terms, commonly referred to as genuine twist-3 TMDs, are defined as [79, 137]

$$\tilde{e}^q(x, k_\perp) = \frac{i}{Mx} \frac{g}{2} \int \frac{dz^- d^2 \vec{z}_\perp}{2(2\pi)^3} e^{ik \cdot z} \times \langle P | \bar{\psi}_+(0) \sigma^{j+} [A_\perp^j(z) - A_\perp^j(0)] \psi_+(z) | P \rangle |_{z^+=0}, \quad (19)$$

$$2xk_\perp^j \tilde{f}^{\perp q}(x, k_\perp) = g \int \frac{dz^- d^2 \vec{z}_\perp}{2(2\pi)^3} e^{ik \cdot z} \times \langle P | \bar{\psi}_+(0) \gamma^+ [A_\perp^j(0) + A_\perp^j(z)] \psi_+(z) | P \rangle |_{z^+=0}. \quad (20)$$

Sum rules serve as a measure of the internal consistency and effectiveness of the model [136]. In this context, the twist-2 and twist-3 PDFs defined as the integrated TMDs, $j(x) = \int d^2 k_\perp j(x, k_\perp)$, with $j(x, k_\perp)$ denoting the TMDs and the PDFs are required to satisfy the following sum rules:

$$\int dx f_1^q(x) = N_q, \quad (21)$$

$$\sum_q \int dx x f_1^q(x) = 1 - \int dx x f_1^g(x), \quad (22)$$

$$\sum_q m_q \int dx e^q(x) = \sigma_K, \quad (23)$$

$$\int dx x e^q(x) = \frac{m_q}{M} N_q. \quad (24)$$

Equation (21) expresses the number sum rule, where N_q denotes the total number of valence quarks of a given flavor [138]. Equation (22) represents the momentum sum rule, which requires that the quark, antiquark, and gluon constituents collectively carry the full light-front momentum of the meson. It is important to note that, due to the explicit k_\perp^j factor in Eq. (14), no corresponding PDF or sum rule exists for the TMD $f^{\perp q}(x, k_\perp)$.

The zeroth moment of $e^q(x)$, given in Eq. (23), contains a singular contribution at $x = 0$ and is related to the kaon's scalar form factor at zero momentum transfer, σ_K [135, 139]. The second sum rule of $e^q(x)$, Eq. (24), can be reformulated as the first-moment sum rule of $\tilde{e}^q(x)$ by employing the twist relations in Eq. (18) together with the number sum rule in Eq. (21).

$$\int dx x \tilde{e}^q(x) = 0. \quad (25)$$

We will examine this sum rule within our model in the next section.

Overlap representations of TMDs

In this subsection, we review the LFWF overlap representations for the leading-twist and subleading-twist TMDs of the kaon. In Fock space, the meson state is expressed as a superposition of all possible Fock components,

$$\begin{aligned} |P\rangle &= \sum_n \sum_{\lambda_1, \lambda_2, \dots, \lambda_n} \int \prod_1^n \frac{[dx_i d^2 p_{\perp i}]}{2(2\pi)^3 \sqrt{x_i}} \\ &\times 2(2\pi)^3 \delta(1 - \sum_1^n x_i) \delta^2(P_\perp - \sum_1^n p_{\perp i}) \\ &\times \Psi_{n, \{\lambda_i\}}(\{x_i, k_{\perp i}\}) |\{x_i P^+, p_{\perp i}, \lambda_i\}\rangle, \end{aligned} \quad (26)$$

where $k_{\perp i}$ and $p_{\perp i}$ represent the relative transverse momentum and physical transverse momentum, respectively, *i.e.*, $k_{\perp i} = p_{\perp i} - x_i P_\perp$. The corresponding orthonormal relation is

$$\langle P' | P \rangle = \sum_{n, n'} 2P^+ (2\pi)^3 \delta^3(P - P') \delta_{nn'} P_n, \quad (27)$$

where $\delta^3(P - P') = \delta(P^+ - P'^+) \delta^2(P_\perp - P'_\perp)$, and P_n defines the probability of finding the n -parton state in the meson. Although the complete expansion includes all Fock states, in this work we restrict our attention to the two lowest components, the two-body LFWF ψ_2 for the $|q\bar{q}\rangle$ state and the three-body LFWF ψ_3 for the $|q\bar{q}g\rangle$ state. Using the model parameters listed in Table I, we find that the probabilities for the $|q\bar{q}\rangle$ and $|q\bar{q}g\rangle$ Fock sectors are 52.64% and 47.36%, respectively.

Using the meson state in Eq. (27) together with the quantized quark and gluon fields in the Lepage-Brodsky prescription [140, 141], the twist-2 quark TMD $f_1^q(x, k_\perp)$

and the twist-3 quark TMDs $\tilde{e}^q(x, k_\perp)$ and $\tilde{f}_\perp^q(x, k_\perp)$ can be expressed in terms of overlaps of the LFWFs as [79]

$$\begin{aligned} f_1^q(x, k_\perp) &= \sum_{\lambda_1, \lambda_2} d[12] \Psi_{2, \lambda_1 \lambda_2}^* \Psi_{2, \lambda_1 \lambda_2} \delta^3(\tilde{p}'_1 - \tilde{k}) \\ &+ \sum_{\lambda_1, \lambda_2, \lambda_g} \int d[123] \Psi_{3, \lambda_1 \lambda_2 \lambda_g}^* \Psi_{3, \lambda_1 \lambda_2 \lambda_g} \delta^3(\tilde{p}_1 - \tilde{k}), \end{aligned} \quad (28)$$

$$\begin{aligned} \tilde{e}^q(x, k_\perp) &= -\frac{g C_F \sqrt{2}}{Mx} \sum_{\lambda_2, \lambda_g} \int d[12] d[123] \frac{2(2\pi)^3}{\sqrt{x_g}} \\ &\times (\Psi_{2, -\lambda_2}^* \Psi_{3, +\lambda_2 \lambda_g} - \Psi_{2, +\lambda_2} \Psi_{3, -\lambda_2 \lambda_g}^*) \\ &\times [\delta^3(\tilde{p}'_1 - \tilde{k}) - \delta^3(\tilde{p}_1 - \tilde{k})] \delta^3(\tilde{p}'_2 - \tilde{p}_2), \end{aligned} \quad (29)$$

$$\begin{aligned} \tilde{f}_\perp^q(x, k_\perp) &= \frac{g C_F \sqrt{2}}{2x k_\perp} \sum_{\lambda_1, \lambda_2, \lambda_g} \int d[12] d[123] \frac{2(2\pi)^3}{\sqrt{x_g}} (-)^{\frac{\lambda_g+1}{2}} \\ &\times [\Psi_{2, \lambda_1 \lambda_2}^* \Psi_{3, \lambda_1 \lambda_2 \lambda_g} \delta^3(\tilde{p}_1 - \tilde{k}) \\ &+ \Psi_{2, \lambda_1 \lambda_2} \Psi_{3, \lambda_1 \lambda_2 \lambda_g}^* \delta^3(\tilde{p}'_1 - \tilde{k})] \delta^3(\tilde{p}'_2 - \tilde{p}_2). \end{aligned} \quad (30)$$

The twist-2 gluon TMD $f_1^g(x, k_\perp)$ is expressed as

$$\begin{aligned} f_1^g(x, k_\perp) &= \sum_{\lambda_1, \lambda_2, \lambda_g} \int d[123] \Psi_{3, \lambda_1 \lambda_2 \lambda_g}^* \Psi_{3, \lambda_1 \lambda_2 \lambda_g} \\ &\times \delta^3(\tilde{p}_g - \tilde{k}). \end{aligned} \quad (31)$$

The conventions we adopt are

$$\begin{aligned} d[12] &\equiv \frac{\prod_1^2 dx'_i d^2 p'_{\perp i}}{[2(2\pi)^3]^2} 2(2\pi)^3 \delta^3(\tilde{P} - \sum_1^2 \tilde{p}'_i), \\ d[123] &\equiv \frac{\prod_1^3 dx_i d^2 p_{\perp i}}{[2(2\pi)^3]^3} 2(2\pi)^3 \delta^3(\tilde{P} - \sum_1^3 \tilde{p}_i), \end{aligned} \quad (32)$$

where $\delta^3(\tilde{P} - \sum_1^n \tilde{p}_i) = \delta(1 - \sum_1^n x_i) \delta^2(P_\perp - \sum_1^n p_{\perp i})$. For simplicity, we omit the arguments $(\tilde{p}'_1, \tilde{p}'_2)$ from the quark-antiquark LFWFs and $(\tilde{p}_1, \tilde{p}_2, \tilde{p}_g)$ from the quark-antiquark-gluon LFWFs, where each momentum is denoted by $\tilde{k} \equiv (x, k_\perp)$. The color factor, $C_F = 2/\sqrt{3}$, derives from the quark-quark-gluon matrix element $\langle q\bar{q} | \Psi_b A^{\mu, a} T_{bc}^a \Psi_c | q\bar{q}g \rangle$ and its hermitian conjugate. As shown in Eqs. (28)-(30), the unpolarized TMD $f_1(x, k_\perp)$ can be decomposed into the individual overlaps of the $|q\bar{q}\rangle$ and $|q\bar{q}g\rangle$ Fock sectors' LFWFs, while the genuine twist-3 TMDs $\tilde{e}(x, k_\perp)$ and $\tilde{f}_\perp(x, k_\perp)$ blend the $|q\bar{q}\rangle$ and the $|q\bar{q}g\rangle$ Fock sectors. This indicates only leading-twist TMDs and PDFs contribute to probabilistic interpretation. The twist-3 TMDs are interpreted as some interference of scattering between a coherent quark-gluon pair and a single quark [135, 139, 142].

IV. NUMERICAL RESULTS

Using the basis truncation parameters $\{N_{\max}, K\} = \{14, 15\}$ summarized in Table I, we solve the light-front

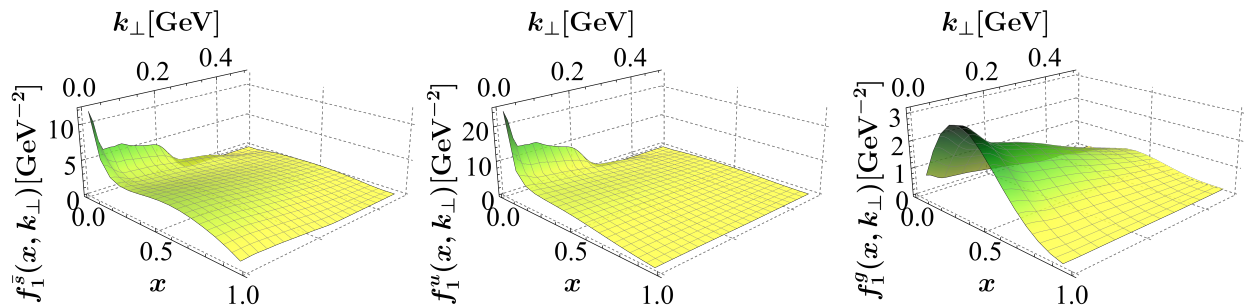


FIG. 1. 3D plots of the BLFQ results for the twist-2 TMD $f_1(x, k_\perp)$ of the kaon. The left, middle, and right panels correspond to the \bar{s} quark, u quark, and gluon, respectively. As described in the text, all results are obtained by averaging over BLFQ calculations with $N_{\max} = \{12, 14, 16\}$ and $K = 15$.

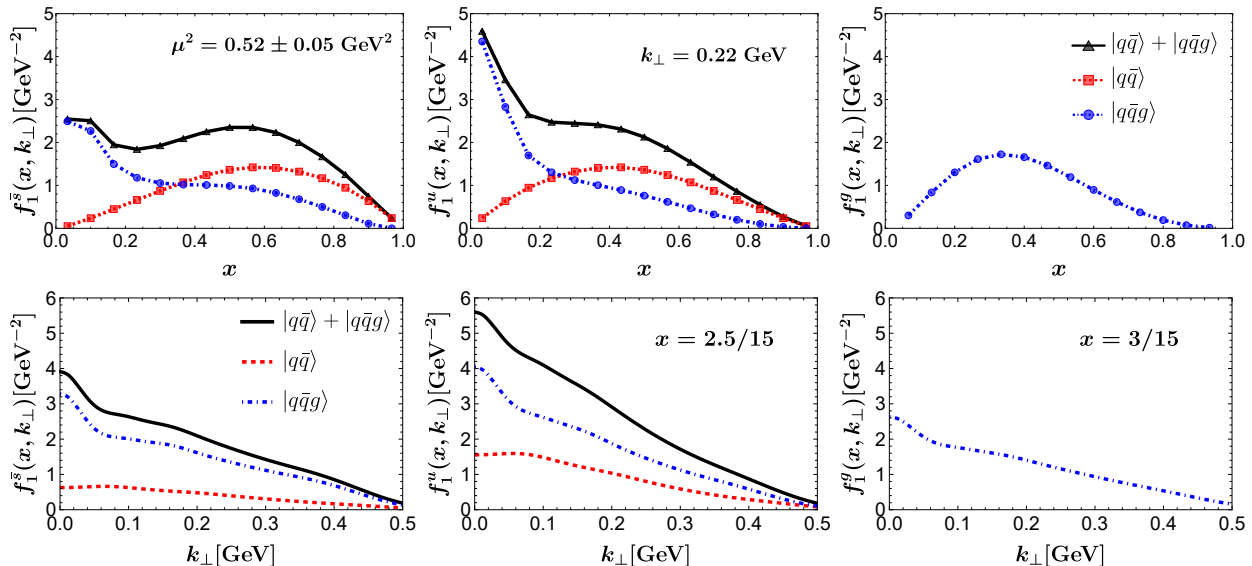


FIG. 2. Contributions from the $|q\bar{q}\rangle$ (red lines) and $|q\bar{q}g\rangle$ (blue lines) Fock sectors to the total (black lines) twist-2 TMD $f_1(x, k_\perp)$ of the kaon. The left, middle, and right panels correspond to the \bar{s} quark, u quark, and gluon, respectively. In the upper panels, the TMDs are shown as functions of x at fixed $k_\perp = 0.22$ GeV. In the lower panels, the TMDs are shown as functions of k_\perp at fixed $x = 2.5/15$ for a quark and $x = 3/15$ for a gluon. As described in the text, all results are obtained by averaging over BLFQ calculations with $N_{\max} = \{12, 14, 16\}$ and $K = 15$.

stationary Schrödinger equation and obtain the two-Fock-sector LFWFs of the kaon, corresponding to a mass $M = 0.485$ GeV. The nonperturbative solutions obtained in single-particle coordinates Eq. (7) are transformed to relative coordinates by factorizing out the center-of-mass motion [88, 94, 99], yielding the boost-invariant LFWFs $\Psi_{n, \{\lambda_i\}}(x_i, p_{\perp i})$. These LFWFs are then employed in the overlap representations, Eqs. (28)–(31), to compute the quark and gluon TMDs and PDFs of the kaon.

The TMDs computed within BLFQ exhibit oscillations in the transverse momentum direction, reflecting the oscillatory behavior of the 2D-HO basis functions used in the transverse plane. The transverse basis states are determined by the transverse truncation parameter N_{\max} and the 2D-HO scale b together. These oscillatory artifacts, arising from the finite basis, can be reduced by

averaging results across different N_{\max} values. Following the procedure of Refs. [79, 95, 99], we perform a two-step averaging at fixed K : first averaging the results obtained at $N_{\max} = n$ and $N_{\max} = n + 2$, then averaging those at $N_{\max} = n + 2$ and $N_{\max} = n + 4$. The final result is obtained by averaging these two intermediate averages, thus incorporating BLFQ outputs at $N_{\max} = \{n, n + 2, n + 4\}$.

A. Twist-2 and twist-3 TMDs

Unlike the pion, the kaon contains a strange quark as one of its valence constituents. Accordingly, we calculate two sets of results for different quark flavors within the $|q\bar{q}\rangle$ and $|q\bar{q}\rangle + |q\bar{q}g\rangle$ Fock sectors. In addition, we also evaluate the leading-twist TMDs and PDFs of the gluon in the $|q\bar{q}g\rangle$ sector.

In Fig. 1, we show the three-dimensional profiles of the unpolarized valence-quark (u and \bar{s}) and gluon leading-twist TMDs, $f_1(x, k_\perp)$, in the kaon. The results are obtained after averaging over N_{\max} in the $|q\bar{q}\rangle + |q\bar{q}g\rangle$ Fock space and are presented as functions of the parton's longitudinal momentum fraction x and transverse momentum k_\perp . The left and middle panels display the total u - and \bar{s} -quark TMDs, which include contributions from both the leading and next-to-leading Fock sectors, while the right panel shows the gluon TMD.

We observe that the BLFQ results exhibit oscillatory behavior that depends on N_{\max} . The oscillation amplitude is more pronounced at small k_\perp and low x , while the oscillation phase varies with changing N_{\max} . By averaging the results obtained at different N_{\max} as described above, we effectively suppress these oscillations, leading to smoother distributions. Here, we present the results for the basis truncation $N_{\max} = \{12, 14, 16\}$ and $K = 15$. In contrast, at large k_\perp and for $x > 0.1$, the oscillation amplitude is already small, indicating better numerical stability of the results in that region.

We find that the TMDs still exhibit small residual oscillations in the k_\perp direction even after averaging. The TMDs drop to zero abruptly in the transverse plane at the ultraviolet (UV) cutoff $\sim b\sqrt{N_{\max}}$. Note that the UV cutoff increases with increasing N_{\max} , and consequently, the fall-off of the TMDs extends to higher transverse momenta for larger N_{\max} . This characteristic behavior of TMDs within our BLFQ framework has also been observed previously for physical spin- $\frac{1}{2}$ particles in QED and for light pseudoscalar particles in QCD, *i.e.*, the electron and the pion, respectively, as reported in Refs. [79, 143].

The quark TMD exhibits a pronounced peak at low x , highlighting the contribution of the next-to-leading Fock sector that includes a dynamical gluon, as shown in Figs. 1 and 2. In contrast, the leading (valence) Fock sector contributes predominantly at intermediate values of x and features a broader distribution in transverse momentum k_\perp . This is illustrated in Fig. 2, where we present two-dimensional slices of the total TMDs, which include contributions from both the leading and next-to-leading Fock sectors, along with their individual components: the leading ($|q\bar{q}\rangle$) and next-to-leading ($|q\bar{q}g\rangle$) sectors. Furthermore, the TMD from the valence sector decreases more slowly at large k_\perp compared to the next-to-leading sector. This slower fall-off indicates that valence quarks are more likely to carry higher transverse momenta, reflecting stronger intrinsic transverse motion in the absence of explicit gluon degrees of freedom. Such momentum-space behavior is consistent with previous phenomenological studies [71, 130, 131, 144–146] and with earlier BLFQ results for the pion [147]. Finally, the strange-quark distribution in the kaon is significantly larger than that of the up quark at large x , indicating that the heavier quark carries a greater fraction of the longitudinal momentum, as expected.

The gluon TMD in the kaon is extracted from the $|q\bar{q}g\rangle$

Fock sector and is shown in the right panels of Figs. 1 and 2. The probability of finding an unpolarized gluon carrying a momentum fraction x in the kaon peaks around $x \approx 0.33$. The distribution is narrower in x than the quark TMD from the valence Fock sector, indicating a more localized gluon momentum structure along the longitudinal direction. We further observe that the probability of finding a gluon is smaller than that of finding a quark in the valence Fock sector at our model scale. Moreover, the overall shape of the gluon TMD is consistent with expectations for an effective massive gluon: it vanishes at both endpoints ($x \rightarrow 0$ and $x \rightarrow 1$) and is concentrated in the intermediate- x region.

Figure 3 shows the total twist-3 TMDs, $e(x, k_\perp)$ and $f^\perp(x, k_\perp)$, obtained using the EOM relations in Eq. (18). Both distributions exhibit similar qualitative behavior, and their magnitudes are larger than that of the leading-twist TMD $f_1(x, k_\perp)$. Their shape is primarily driven by the function $f_1(x, k_\perp)/x$, which is singular at $x = 0$. Nevertheless, the contributions of twist-3 TMDs to physical cross sections are suppressed by a factor of M/P^+ [47], and thus higher-twist effects are reduced in high-energy processes. In addition, the twist-3 TMDs decrease rapidly with increasing transverse momentum. As noted earlier, twist-3 TMDs do not admit a probabilistic interpretation. These distributions are inherently multi-parton in nature, arising from the interference between different Fock sectors and encoding the dynamics of quark–quark–gluon correlations.

Figure 4 presents the genuine twist-3 TMDs, $\tilde{e}(x, k_\perp)$ and $\tilde{f}^\perp(x, k_\perp)$. These distributions also display similar qualitative behavior, and their magnitudes are comparable to that of the leading-twist TMD $f_1(x, k_\perp)$. Both the valence quarks \bar{s} and u in the kaon show similar qualitative patterns, although the magnitude of the u -quark distribution is larger than that of the \bar{s} -quark. This is further illustrated in Fig. 5, where the two-dimensional slices of the genuine twist-3 TMDs are presented. An analysis of the operator structures in the twist-2 correlators indicates that twist-2 TMDs admit a probabilistic interpretation [7, 21, 40, 148, 149]. In contrast, genuine twist-3 TMDs do not have such an interpretation; rather, they correspond to unpolarized interference distributions [49].

The total twist-3 TMDs, $e(x, k_\perp)$ and $f^\perp(x, k_\perp)$, which include contributions from both the twist-2 and genuine twist-3 terms, are shown in Fig. 6 as functions of x for three different values of k_\perp . The same figure also displays the individual contributions from the twist-2 and genuine twist-3 components. We observe that the twist-2 contribution strongly dominates over the genuine twist-3 contribution. As a result, the overall behavior of the total twist-3 TMDs closely follows that of the twist-2 contribution, as evident from Fig. 6.

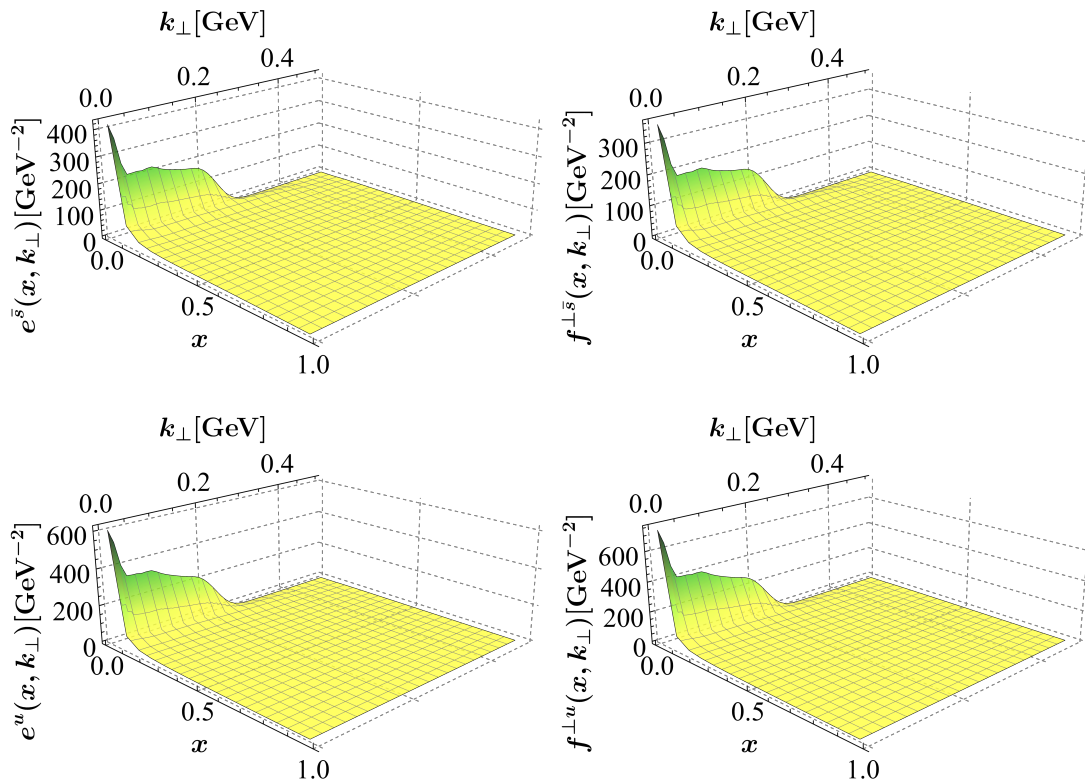


FIG. 3. 3D plots of the BLFQ results for the twist-3 TMDs $e(x, k_{\perp})$ (left panels) and $f^{\perp}(x, k_{\perp})$ (right panels). The upper panels correspond to the \bar{s} quark, while the lower panels correspond to the u quark. As described in the text, all results are obtained by averaging over BLFQ calculations with $N_{\max} = \{12, 14, 16\}$ and $K = 15$. Note the differences in the vertical scales.

B. k_{\perp} moments of the TMDs

We define the x -dependent mean squared transverse momentum of a parton as [79, 105]

$$\langle k_{\perp}^2 \rangle_{f_1}(x) = \frac{\int d^2 k_{\perp} k_{\perp}^2 f_1(x, k_{\perp})}{\int d^2 k_{\perp} f_1(x, k_{\perp})}. \quad (33)$$

In Fig. 7, we present the x -dependence of the mean squared transverse momentum, $\langle k_{\perp}^2 \rangle_{f_1}(x)$, for the valence quarks (u and \bar{s}) and the gluon in the kaon, computed within the Fock components $|q\bar{q}\rangle + |q\bar{q}g\rangle$. Within the BLFQ framework, $\langle k_{\perp}^2 \rangle_{f_1}(x)$ exhibits a visible flavor and x dependence. Due to flavor symmetry breaking arising from the mass difference between the u and \bar{s} quarks, the peak of $\langle k_{\perp}^2 \rangle_{f_1}(x)$ is shifted away from $x = 0.5$. The shift occurs towards higher x for the u quark and lower x for the \bar{s} quark. Qualitatively, our results are consistent with experimental extractions that account for the x -dependence of $\langle k_{\perp}^2 \rangle$, such as those reported in Refs. [150, 151]. The correlation between the gluon's transverse and longitudinal momenta in the kaon is shown in the right panel of Fig. 7. The $\langle k_{\perp}^2 \rangle_{f_1}(x)$ for the gluon is approximately symmetric about $x = 0.5$, exhibiting a relatively larger value in the intermediate- x region and decreasing rapidly at both small and large

x . The results indicate that the k_{\perp} moments of quarks and gluons are very similar across the entire range of the momentum fraction x .

Our calculations do not support the commonly used x - k_{\perp} factorization ansatz often adopted in preliminary phenomenological studies [152–157]. In particular, the nontrivial x dependence of $\langle k_{\perp}^2 \rangle_{f_1}$ prevents the factorization of the TMD in the form

$$f_1^q(x, k_{\perp}) = f_1^q(x) \frac{\hat{f}_1^q(k_{\perp})}{\mathcal{N}}, \quad (34)$$

where $\mathcal{N} = \int d^2 k_{\perp} \hat{f}_1^q(k_{\perp})$.

TABLE II. The first moment $\langle k_{\perp} \rangle$ (in GeV) and the square root of second moment $\langle k_{\perp}^2 \rangle^{1/2}$ (in GeV) of the quark (twist-2 and twist-3) and gluon (twist-2) TMDs in the kaon are obtained by averaging over the basis truncation parameters $N_{\max} = \{12, 14, 16\}$ truncation and $K = 15$ as described in the text.

| TMDs | $\langle k_{\perp} \rangle_u$ | $\langle k_{\perp} \rangle_{\bar{s}}$ | $\langle k_{\perp}^2 \rangle_u^{1/2}$ | $\langle k_{\perp}^2 \rangle_{\bar{s}}^{1/2}$ | $\langle k_{\perp} \rangle_g$ | $\langle k_{\perp}^2 \rangle_g^{1/2}$ |
|-------------|-------------------------------|---------------------------------------|---------------------------------------|---|-------------------------------|---------------------------------------|
| f_1 | 0.28 | 0.29 | 0.31 | 0.32 | 0.30 | 0.34 |
| e | 0.20 | 0.23 | 0.25 | 0.27 | - | - |
| f^{\perp} | 0.20 | 0.23 | 0.24 | 0.27 | - | - |

Although twist-3 TMDs e and f^{\perp} do not admit a prob-

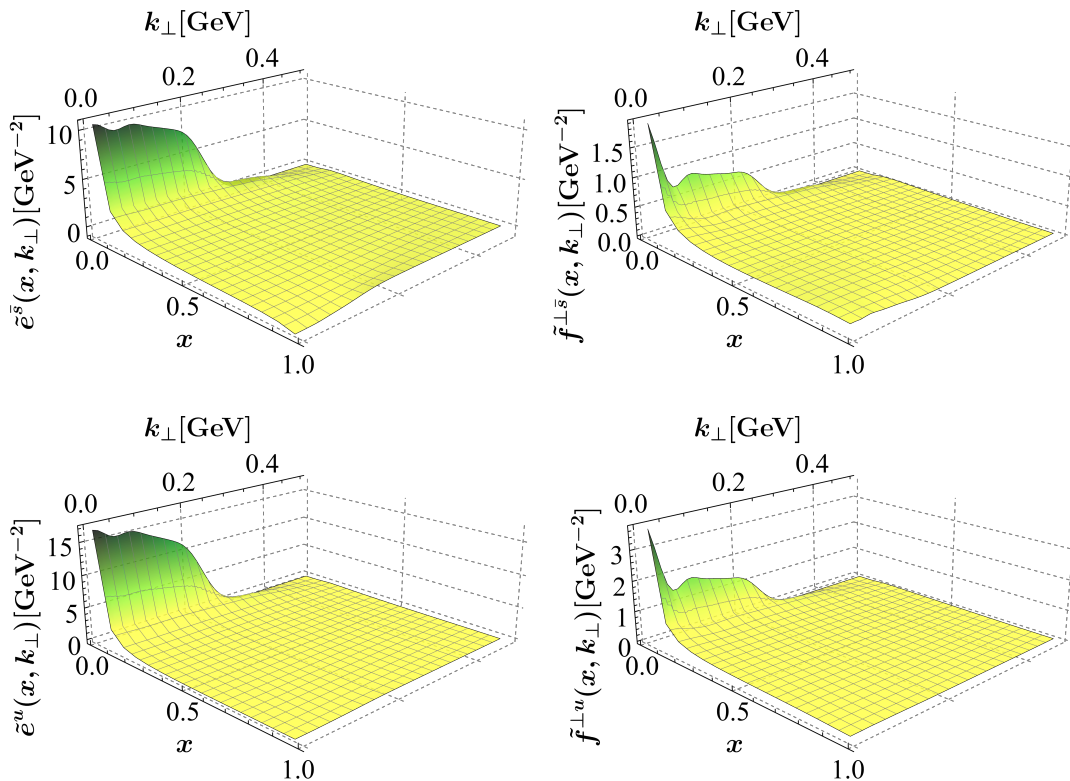


FIG. 4. 3D plots of the BLFQ results for the genuine twist-3 TMDs $\tilde{e}(x, k_{\perp})$ (left panels) and $\tilde{f}^{\perp}(x, k_{\perp})$ (right panels). The upper panels correspond to the \bar{s} quark, while the lower panels correspond to the u quark. As described in the text, all results are obtained by averaging over BLFQ calculations with $N_{\max} = \{12, 14, 16\}$ and $K = 15$.

abilistic interpretation, we compute their first and second transverse-momentum moments, defined as [63]

$$\langle k_{\perp}^n \rangle_{\text{TMD}} = \frac{\int dx \int d^2 k_{\perp} k_{\perp}^n \text{TMD}}{\int dx \int d^2 k_{\perp} \text{TMD}}. \quad (35)$$

The corresponding results are summarized in Table II.

C. Twist-2 and twist-3 PDFs

In this subsection, we focus on the integrated TMDs over the transverse momentum k_{\perp} , namely the PDFs. The leading-twist unpolarized PDFs $f_1(x)$ for the valence quarks, including contributions from both the leading and next-to-leading Fock sectors, are presented in the left (\bar{s} quark) and middle (u quark) panels of Fig. 8. The separate contributions from the $|q\bar{q}\rangle$ and $|q\bar{q}g\rangle$ Fock components are also shown in the same plots. As seen in Fig. 8, the inclusion of a dynamical gluon leads to a noticeable enhancement of the quark PDFs in the small- x region, reflecting the natural onset of gluon effects through higher Fock components in our framework. At small x , the u distribution is slightly larger than that of the \bar{s} quark, whereas in the large- x region it becomes smaller. Within the valence Fock sector $|q\bar{q}\rangle$, the PDFs

exhibit features consistent with previous model calculations and phenomenological analyses.

The gluon PDF, shown in the right panel of Fig. 8, is narrower in x compared to the quark PDFs and therefore exhibits a more pronounced peak. This narrower shape arises from the larger effective gluon mass in our model, which suppresses contributions at small and large x and concentrates the distribution around intermediate x .

As shown in Fig. 9, the genuine twist-3 function $x\tilde{e}(x)$ is positive for $x < 0.5$ and negative for $x > 0.5$, while $x\tilde{f}^{\perp}(x)$ remains positive over the entire x range. Figure 10 shows the total twist-3 PDFs along with their decomposition into the twist-2 contribution and the genuine twist-3 parts. We note that the magnitude of the twist-2 contribution is significantly larger than that of the genuine twist-3 components.

We also find that the integrated value of $x\tilde{e}(x)$ over x vanishes, demonstrating that our BLFQ results correctly satisfy the sum rule defined in Eq. (25). This sum rule originates from the EOM relations and is therefore expected to hold universally. Our findings are consistent with previous BLFQ studies of $\tilde{e}(x)$ for the pion [79] and proton [158], both of which satisfy the same sum rule. For comparison, the calculation of $\tilde{e}(x)$ for the nucleon in Ref. [72], which includes $|qqq\rangle$ and $|qqqg\rangle$ Fock components, does not fulfill the sum rule in Eq. (25). This may

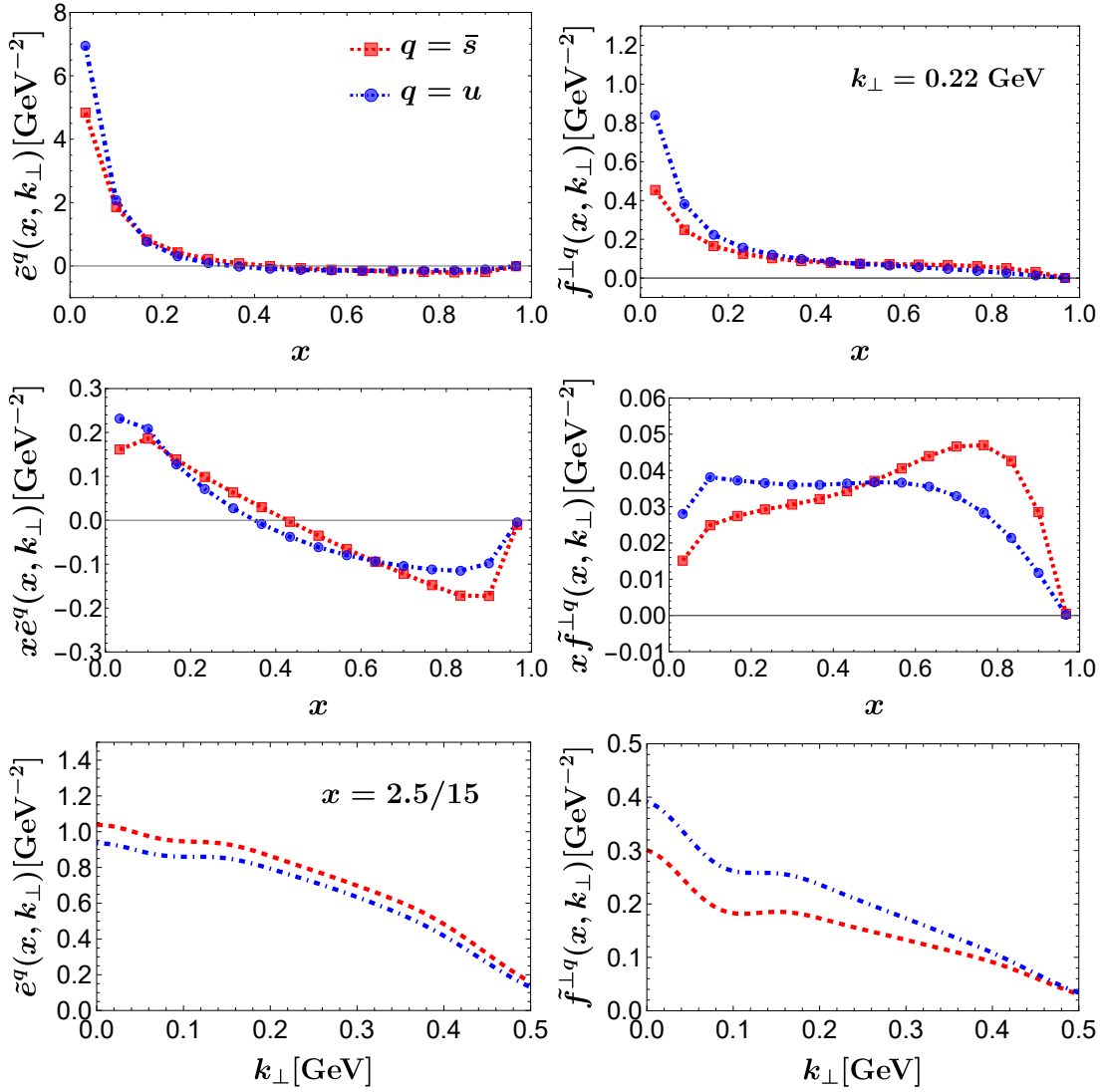


FIG. 5. 2D slices of the 3D BLFQ results for the genuine twist-3 TMDs $\tilde{e}(x, k_\perp)$ (left panels) and $\tilde{f}^\perp(x, k_\perp)$ (right panels). In the upper panels, the TMDs are shown as functions of x at fixed $k_\perp = 0.22$ GeV. In the middle panel, the TMDs $x\tilde{e}(x, k_\perp)$ and $x\tilde{f}(x, k_\perp)$ are shown as functions of x with the same fixed k_\perp . In the lower panels, the TMDs are shown as functions of k_\perp at fixed $x = 2.5/15$. The red and blue curves correspond to the \bar{s} and u quarks, respectively. As described in the text, all results are obtained by averaging over BLFQ calculations with $N_{\max} = \{12, 14, 16\}$ and $K = 15$.

arise from neglecting zero modes and truncating the Fock sectors [72]. In contrast, Ref. [75] reports a dressed-quark calculation of $e(x)$ and $\tilde{e}(x)$ at one loop, where $\tilde{e}(x)$ does satisfy the first-moment sum rule (25).

Finally, using the sum rule defined in Eq. (23), we compute the kaon scalar form factor at zero momentum transfer from our BLFQ results, obtaining $\sigma_K = 7.5$ GeV.

Figure 11 (upper panel) shows the ratios of the kaon to pion distributions for both the PDFs and TMDs of the u quark under the initial scale, $\mu_{0\pi}^2 = 0.43 \pm 0.04$ GeV² for the pion and $\mu_{0K}^2 = 0.52 \pm 0.05$ GeV² for the kaon [82, 96, 147]¹. These ratios provide indirect experimen-

tal constraints on the partonic structure of the kaon. For the pion distributions, we use our results obtained from the same light-front QCD Hamiltonian including the $|q\bar{q}\rangle$ and $|q\bar{q}g\rangle$ Fock sectors [147]. For the PDFs, the u -quark distribution in the kaon is nearly identical to that in the pion around $x \approx 0.1$. In the intermediate region $0.1 < x < 0.5$, the kaon distribution is larger, whereas it becomes smaller for $x > 0.5$. This pattern indicates that the u quark in the kaon predominantly populates lower- x regions, while in the pion it tends to carry a larger fraction of the longitudinal momentum. The mid-

¹ We note here a correction for the model scale of the kaon which

is $\mu_{0,K}^2 = 0.52$ GeV² for Phys.Lett.B 868 (2025) 139654 [82].

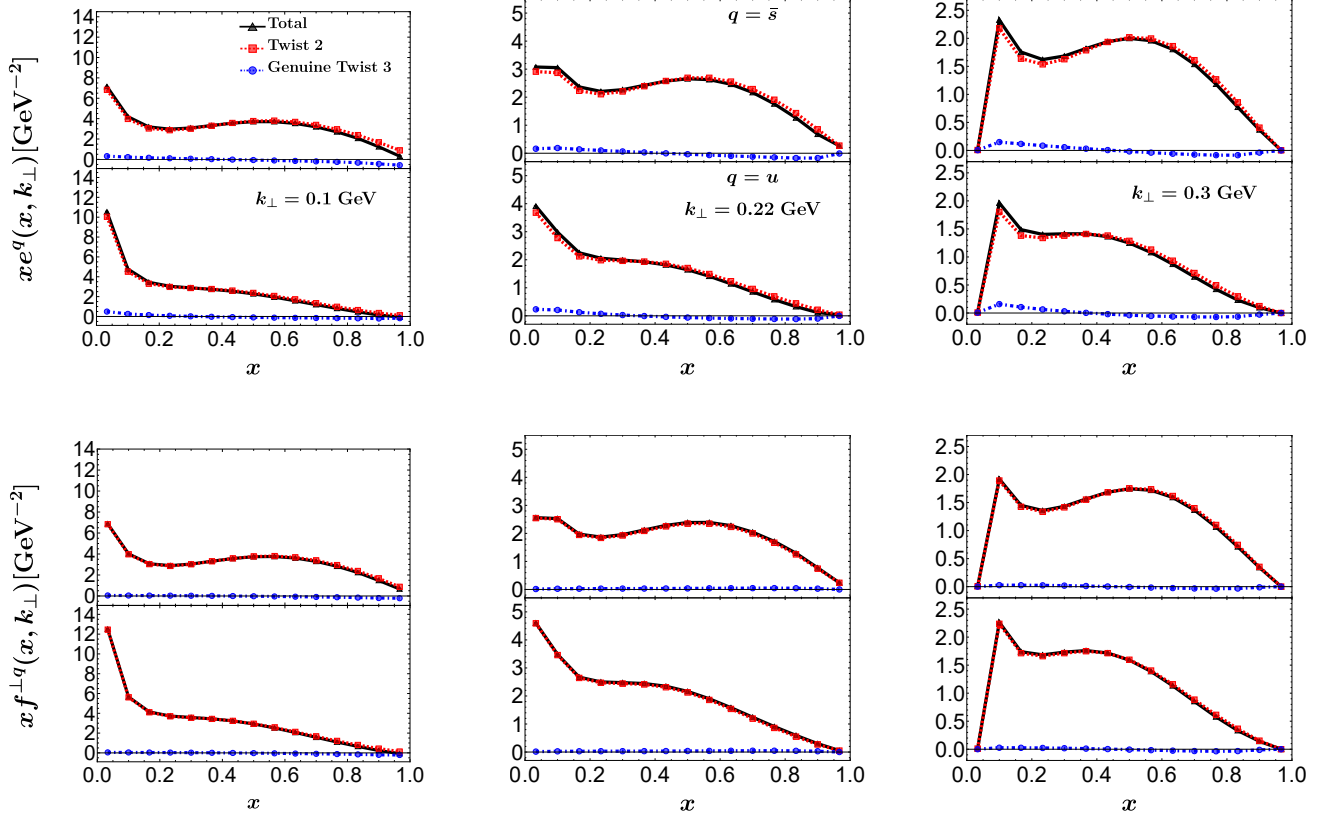


FIG. 6. The total twist-3 TMDs (black curves), the genuine twist-3 contributions (blue curves), and the twist-2 contributions (red curves) shown as functions of x for three different values of k_\perp . The upper and lower panels correspond to the TMDs $e(x, k_\perp)$ and $f^\perp(x, k_\perp)$, respectively. As described in the text, the results are obtained in the BLFQ framework by averaging over truncation parameters $N_{\max} = \{12, 14, 16\}$ with $K = 15$.

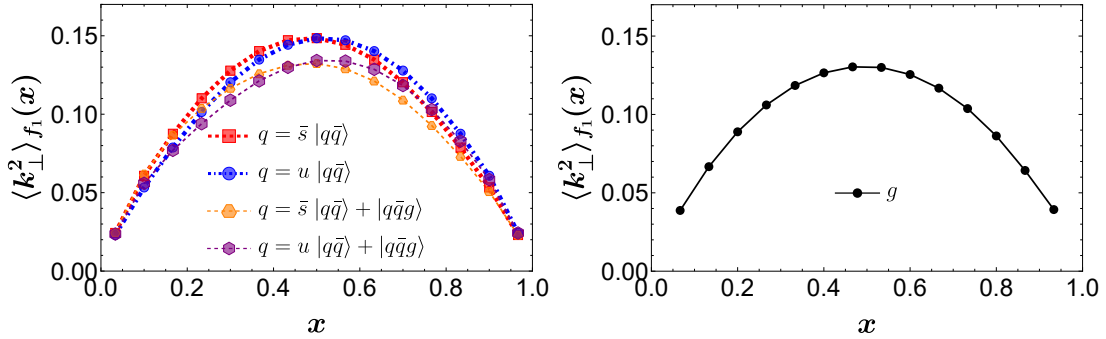


FIG. 7. The x -dependent mean squared transverse momentum of quarks (left panel) for the leading Fock sector $|q\bar{q}\rangle$ and for the combined Fock sectors $|q\bar{q}\rangle + |q\bar{q}g\rangle$, and of gluons (right panel). As described in the text, the results are obtained in the BLFQ framework by averaging over truncation parameters $N_{\max} = \{12, 14, 16\}$ with $K = 15$.

dle panel shows the ratio of the \bar{s} quark to the u quark in the kaon. From these two figures, the strange quark has a larger longitudinal momentum fraction than the light quark in the larger x region.

In contrast, the TMD ratios show that as k_\perp increases, the momentum fraction x carried by the u quark in the kaon shifts toward the larger- x region. This reflects the

nontrivial interplay between the longitudinal and transverse momentum distributions.

The lower panel of Fig. 11 displays the ratios of the kaon to pion distributions for the gluon PDFs and TMDs. Except in the region $0.2 < x < 0.4$, where the gluon distributions in the kaon and pion are nearly identical, the pion gluon distribution dominates in both the small-

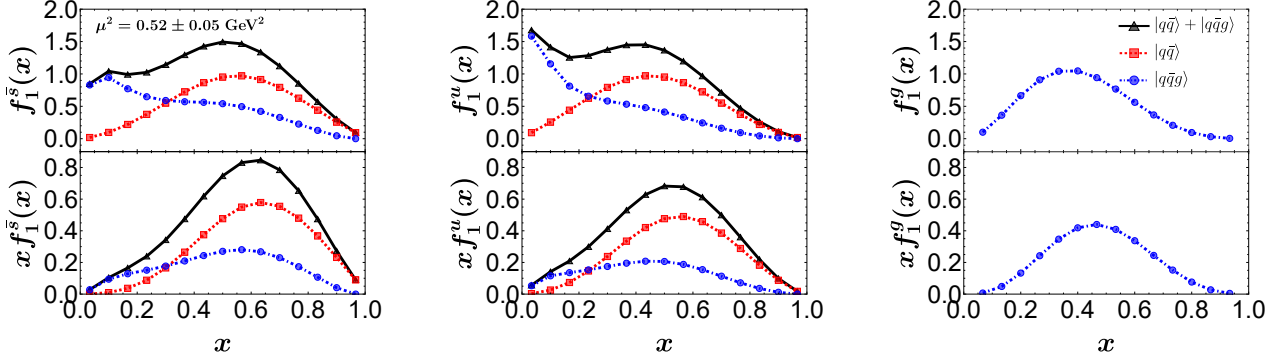


FIG. 8. Contributions from the $|q\bar{q}\rangle$ (red lines) and $|q\bar{q}g\rangle$ (blue lines) Fock sectors to the total (black lines) twist-2 PDFs $f_1(x)$ of the kaon. The left, middle, and right panels correspond to the \bar{s} quark, u quark, and gluon, respectively. As described in the text, all results are obtained by averaging over BLFQ calculations with $N_{\max} = \{12, 14, 16\}$ and $K = 15$.

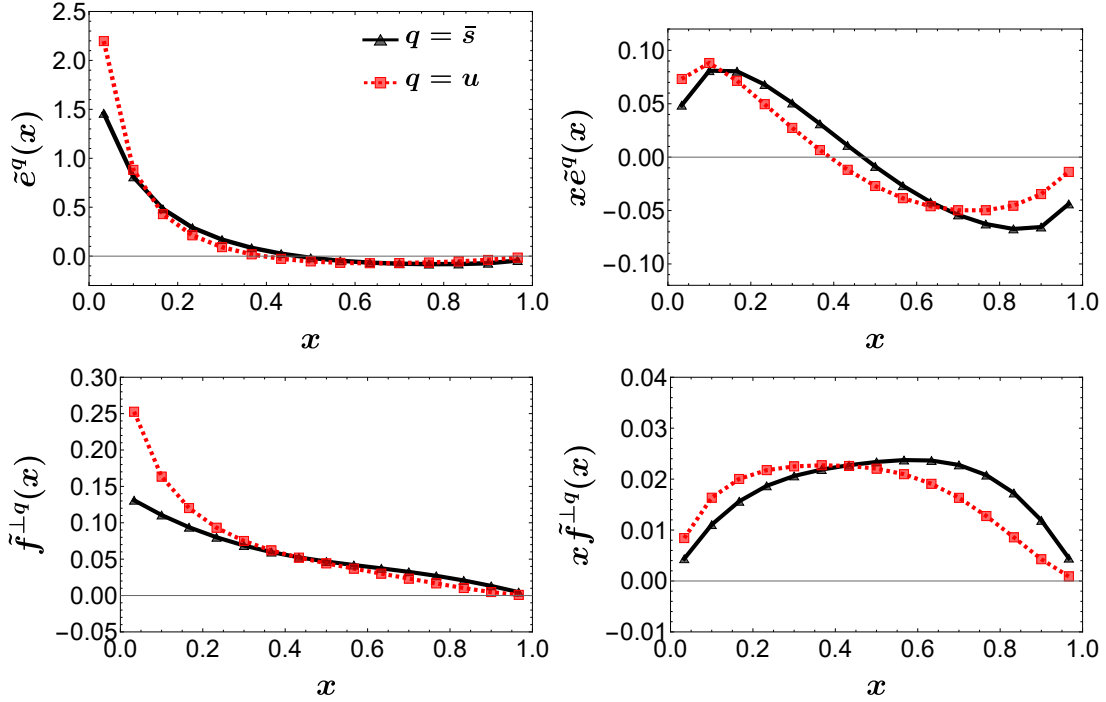


FIG. 9. The results of the genuine twist-3 PDFs $\tilde{e}^q(x)$, $\tilde{f}^{\perp q}(x)$ and $x\tilde{e}^q(x)$, $x\tilde{f}^{\perp q}(x)$ with the different quarks \bar{s} and u of the kaon. As described in the text, all results are acquired by averaging through BLFQ approach with $N_{\max} = \{12, 14, 16\}$ and $K = 15$.

and large- x regions. Meanwhile, the TMD ratios reveal that as k_{\perp} increases, the gluon TMD in the kaon becomes larger in the intermediate- x range ($0.1 < x < 0.5$).

Figure 12 presents our results for kaon PDFs after QCD evolution at NNLO [7, 159, 160]. In the upper panel, we compare the ratios u_v^K/u_v^{π} and \bar{s}_v^K/u_v^{π} with the recent global analysis by the JAM Collaboration [116] at the scale $\mu^2 = 4 \text{ GeV}^2$, which incorporates both experimental data and lattice QCD constraints. The uncertainty bands in our evolved distributions reflect a $\pm 10\%$ uncertainty in the model input scales for the kaon and

pion. These initial scales were fixed by matching the evolved first moments of the valence quark and antiquark distributions to global QCD analyses.

Our results show good agreement with the JAM analysis, reproducing the characteristic decrease of the u_v^K/u_v^{π} ratio and the increase of the \bar{s}_v^K/u_v^{π} ratio with increasing x . The lower-left panel of Fig. 12 compares the ratio of the evolved gluon distributions in the kaon and pion with the corresponding ratio at the initial scale. We observe that, although at the initial scale the kaon's gluon distribution is smaller than that of the pion at both small and

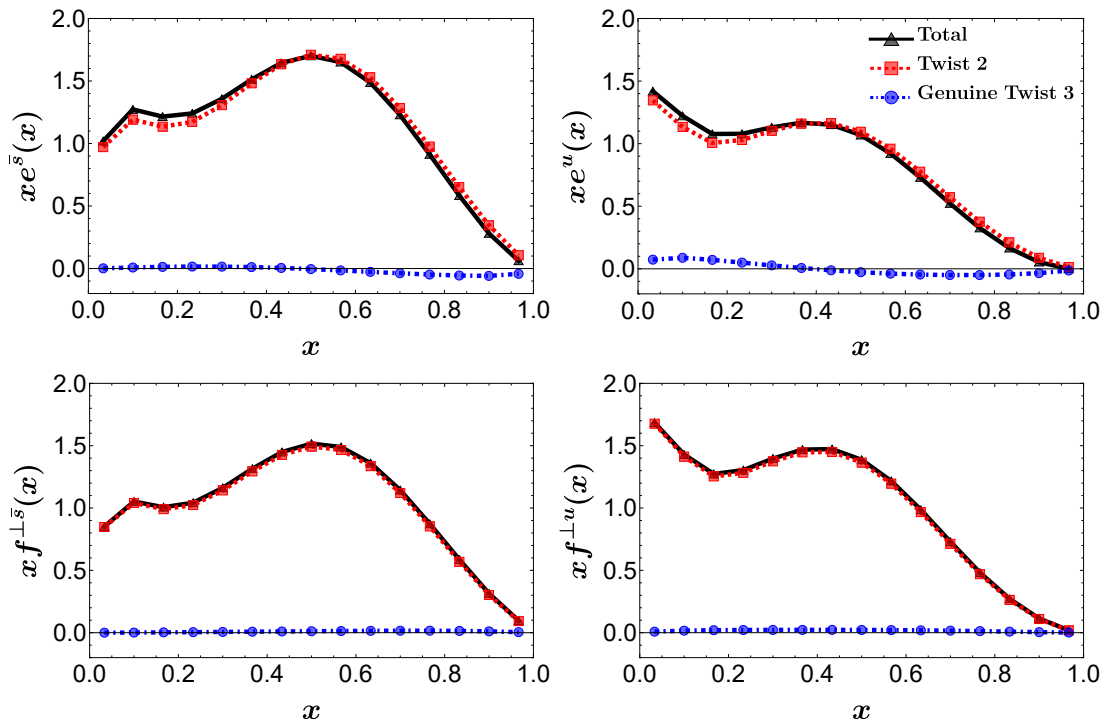


FIG. 10. The total twist-3 PDFs (black curves), the genuine twist-3 contributions (blue curves), and the twist-2 contributions (red curves). The upper and lower panels correspond to the PDFs $e(x)$ and $f^\perp(x)$, respectively. The results are obtained in the BLFQ framework by averaging over truncation parameters $N_{\max} = \{12, 14, 16\}$ with $K = 15$.

large x , QCD evolution drives the two distributions toward very similar behavior. Finally, the lower-right panel presents a direct comparison of our BLFQ results with the JAM 2025 analysis [116] for the quark flavor distributions in the kaon and pion at $\mu^2 = 4 \text{ GeV}^2$. Overall, our findings are in good agreement with the global QCD analysis by the JAM Collaboration.

V. CONCLUSION AND OUTLOOK

In this work, we have investigated the partonic structure of the kaon by computing its leading-twist TMD $f_1(x, k_\perp)$ for both quarks and gluons, and, for the first time, the genuine twist-3 TMDs $\tilde{e}(x, k_\perp)$ and $\tilde{f}^\perp(x, k_\perp)$ for quarks, using light-front wave functions obtained within the Basis Light-Front Quantization (BLFQ) framework. These wave functions are derived from the eigenvectors of the light-front QCD Hamiltonian in the light-cone gauge, incorporating both the $|q\bar{q}\rangle$ and $|q\bar{q}g\rangle$ Fock sectors, together with a three-dimensional confining potential in the leading Fock sector.

Using model-independent equations-of-motion (EOM) relations, we constructed the total twist-3 transverse-momentum-dependent distributions (TMDs) $e(x, k_\perp)$ and $f^\perp(x, k_\perp)$. In this study, the gauge link was set to unity, allowing us to focus exclusively on time-reversal-even (T-even) TMDs. To reduce artifacts arising from

basis truncation, an averaging procedure was applied to the BLFQ results. The integrated TMDs exhibit good numerical stability with respect to basis truncation, and the resulting twist-3 PDFs $e(x)$ satisfy the expected momentum sum rule.

We find that the genuine twist-3 contributions display a distinct x -dependence compared with the twist-2 terms, while their overall magnitude remains subdominant. The twist-2 PDFs, $f_1^q(x)$ obtained in this work are in good agreement with the recent global analysis by the JAM Collaboration [116], which incorporates both experimental data and lattice QCD constraints.

Our results also highlight the important role of dynamical gluons, particularly at small x , where they significantly enhance the quark distributions. We have computed the first moments of the kaon PDFs, providing a clear decomposition of the longitudinal momentum among valence quarks and gluons. Moreover, a comparison of the kaon and pion TMDs reveals characteristic differences in the momentum distribution of the u quark and gluon, offering valuable insights into flavor symmetry breaking in light mesons.

The present work focuses on the T-even distributions. Since the genuine twist-3 and T-odd TMDs share similar operator structures, our results pave the way for future studies of T-odd observables, such as the Boer–Mulders function h_1^\perp in the kaon and its impact on spin asymmetries in Drell–Yan processes. In addition, a detailed investigation of the gluon TMDs and their evolution prop-

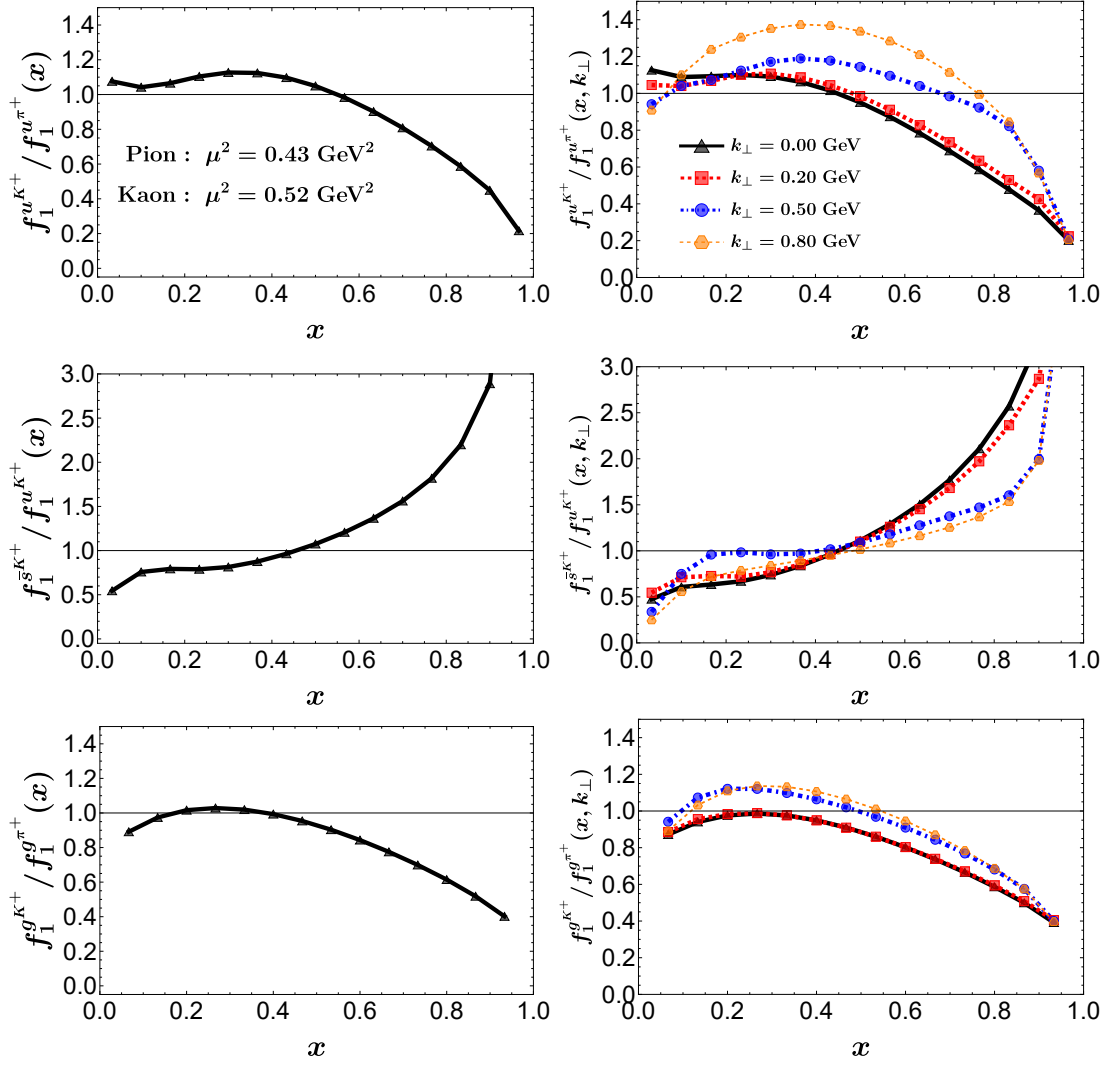


FIG. 11. Ratios of parton distributions. Upper panels: ratio of the up-quark distribution in the kaon to that in the pion. Middle panels: ratio of the strange-quark distribution to the up-quark distribution in the kaon. Lower panels: ratio of the gluon distribution in the kaon to that in the pion. The right and left panels show the TMDs and collinear PDFs, respectively. The TMD ratios are presented for different values of k_{\perp} .

erties within the BLFQ framework will be presented in future work.

We believe that these results, including the twist-3 TMDs, provide valuable predictions for future experimental programs, such as precise measurements of kaon-induced Drell–Yan processes by COMPASS++/AMBER at CERN and forthcoming studies of the 3D structure of the kaon at facilities like the EIC and EicC [161]. Such measurements will offer critical opportunities to refine our understanding of the kaon’s three-dimensional partonic structure and its internal QCD correlations.

ACKNOWLEDGEMENTS

We thank Zhi Hu, Jiatong Wu, and Jialin Chen for many helpful discussions. This work is supported by

National Natural Science Foundation of China, Grant No. 12375143 and 12305095. Z. Z. is supported by China Association for Science and Technology. C. M. is supported by new faculty start up funding by the Institute of Modern Physics, Chinese Academy of Sciences, Grant No. E129952YR0. J. L. is supported by the Special Research Assistant Funding Project, Chinese Academy of Sciences, by the National Science Foundation of Gansu Province, China, Grant No. 23JRRA631. X. Z. is supported by National Natural Science Foundation of China, Grant No. 12375143, by new faculty startup funding by the Institute of Modern Physics, Chinese Academy of Sciences, by Key Research Program of Frontier Sciences, Chinese Academy of Sciences, Grant No. ZDBS-LY-7020, by the Foundation for Key Talents of Gansu Province, by the Central Funds Guiding the Local Science and Technology Development of

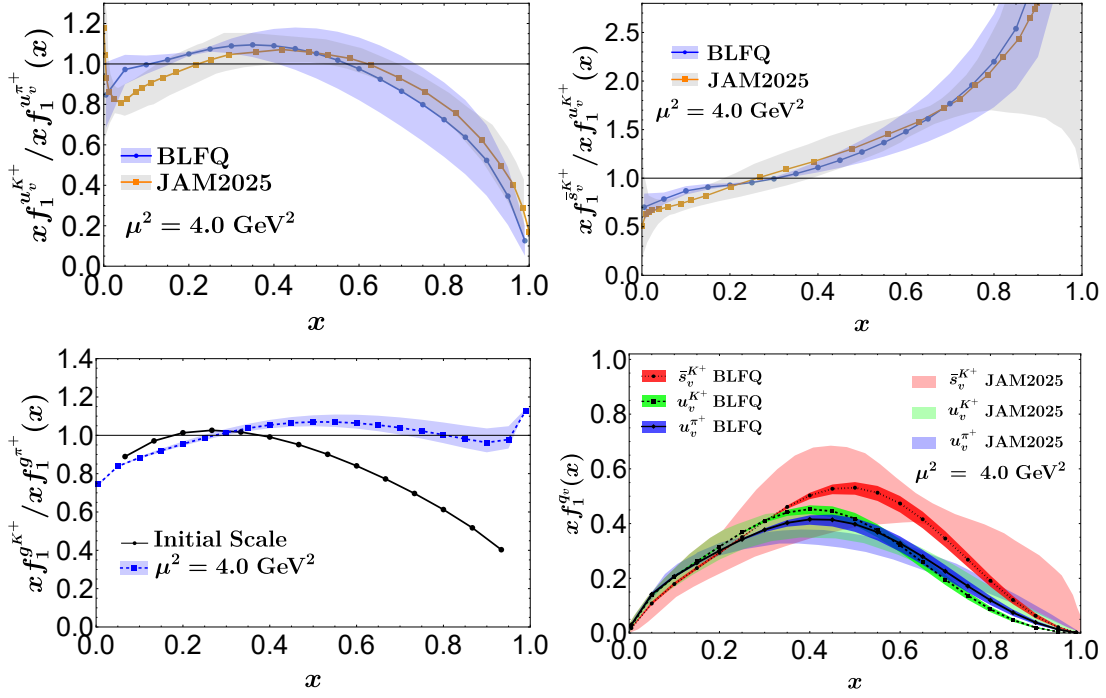


FIG. 12. Kaon PDFs after QCD evolution to $\mu^2 = 4 \text{ GeV}^2$. Upper-left panel: ratio of the up-quark distribution in the kaon to that in the pion. Upper-right panel: ratio of the strange-quark distribution to the up-quark distribution in the kaon. Lower-left panel: ratio of the gluon distribution in the kaon to that in the pion. Lower-right panel: valence-quark distributions in the kaon and pion. Our quark distributions and their ratios are compared with the recent global analysis by the JAM Collaboration [116].

Gansu Province, Grant No. 22ZY1QA006, by Gansu International Collaboration and Talents Recruitment Base of Particle Physics (2023-2027), by International Partnership Program of the Chinese Academy of Sciences, Grant No. 016GJHZ2022103FN, by National Key R & D Program of China, Grant No. 2023YFA1606903 and by the Strategic Priority Research Program of the Chinese

Academy of Sciences, Grant No. XDB34000000. J. P. V. is supported by the Department of Energy under Grant No. DE-SC0023692. A portion of the computational resources were also provided by Advanced Computing Center in Taiyuan and by Sugon Computing Center in Xi'an.

-
- [1] A. Accardi, et al., Electron Ion Collider: The Next QCD Frontier: Understanding the glue that binds us all, *Eur. Phys. J. A* 52 (9) (2016) 268. [arXiv:1212.1701](#), [doi:10.1140/epja/i2016-16268-9](#).
 - [2] A. Bacchetta, M. Diehl, K. Goeke, A. Metz, P. J. Mulders, M. Schlegel, Semi-inclusive deep inelastic scattering at small transverse momentum, *JHEP* 02 (2007) 093. [arXiv:hep-ph/0611265](#), [doi:10.1088/1126-6708/2007/02/093](#).
 - [3] A. V. Belitsky, X. Ji, F. Yuan, Final state interactions and gauge invariant parton distributions, *Nucl. Phys. B* 656 (2003) 165–198. [arXiv:hep-ph/0208038](#), [doi:10.1016/S0550-3213\(03\)00121-4](#).
 - [4] H.-L. Lai, M. Guzzi, J. Huston, Z. Li, P. M. Nadolsky, J. Pumplin, C. P. Yuan, New parton distributions for collider physics, *Phys. Rev. D* 82 (2010) 074024. [arXiv:1007.2241](#), [doi:10.1103/PhysRevD.82.074024](#).
 - [5] J. Pumplin, D. R. Stump, J. Huston, H. L. Lai, P. M. Nadolsky, W. K. Tung, New generation of parton distributions with uncertainties from global QCD analysis, *JHEP* 07 (2002) 012. [arXiv:hep-ph/0201195](#), [doi:10.1088/1126-6708/2002/07/012](#).
 - [6] M. Diehl, Generalized parton distributions, *Phys. Rept.* 388 (2003) 41–277. [arXiv:hep-ph/0307382](#), [doi:10.1016/j.physrep.2003.08.002](#).
 - [7] J. Collins, *Foundations of Perturbative QCD*, Vol. 32, Cambridge University Press, 2011. [doi:10.1017/9781009401845](#).
 - [8] M. Diehl, D. Ostermeier, A. Schafer, Elements of a theory for multiparton interactions in QCD, *JHEP* 03 (2012) 089, [Erratum: *JHEP* 03, 001 (2016)]. [arXiv:1111.0910](#), [doi:10.1007/JHEP03\(2012\)089](#).
 - [9] J. C. Collins, L. Frankfurt, M. Strikman, Factorization for hard exclusive electroproduction of mesons in QCD, *Phys. Rev. D* 56 (1997) 2982–3006. [arXiv:hep-ph/9611433](#), [doi:10.1103/PhysRevD.56.2982](#).
 - [10] T. C. Rogers, An overview of transverse-momentum-dependent factorization and evolution, *Eur. Phys. J. A* 52 (6) (2016) 153. [arXiv:1509.04766](#), [doi:10.1140/epja/i2016-16153-7](#).

- [11] G. F. Sterman, Partons, factorization and resummation, TASI 95, in: Theoretical Advanced Study Institute in Elementary Particle Physics (TASI 95): QCD and Beyond, 1995, pp. 327–408. [arXiv:hep-ph/9606312](#).
- [12] J. C. Collins, D. E. Soper, G. F. Sterman, Factorization for Short Distance Hadron - Hadron Scattering, Nucl. Phys. B 261 (1985) 104–142. [doi:10.1016/0550-3213\(85\)90565-6](#).
- [13] J. C. Collins, D. E. Soper, The Theorems of Perturbative QCD, Ann. Rev. Nucl. Part. Sci. 37 (1987) 383–409. [doi:10.1146/annurev.ns.37.120187.002123](#).
- [14] J. C. Collins, Hard scattering factorization with heavy quarks: A General treatment, Phys. Rev. D 58 (1998) 094002. [arXiv:hep-ph/9806259](#), [doi:10.1103/PhysRevD.58.094002](#).
- [15] V. L. Chernyak, A. R. Zhitnitsky, Asymptotic Behavior of Exclusive Processes in QCD, Phys. Rept. 112 (1984) 173. [doi:10.1016/0370-1573\(84\)90126-1](#).
- [16] D. Müller, D. Robaschik, B. Geyer, F. M. Dittes, J. Hořejši, Wave functions, evolution equations and evolution kernels from light ray operators of QCD, Fortsch. Phys. 42 (1994) 101–141. [arXiv:hep-ph/9812448](#), [doi:10.1002/prop.2190420202](#).
- [17] B. Lampe, E. Reya, Spin physics and polarized structure functions, Phys. Rept. 332 (2000) 1–163. [arXiv:hep-ph/9810270](#), [doi:10.1016/S0370-1573\(99\)00100-3](#).
- [18] E. V. Shuryak, Quantum Chromodynamics and the Theory of Superdense Matter, Phys. Rept. 61 (1980) 71–158. [doi:10.1016/0370-1573\(80\)90105-2](#).
- [19] O. Hen, G. A. Miller, E. Piasetzky, L. B. Weinstein, Nucleon-Nucleon Correlations, Short-lived Excitations, and the Quarks Within, Rev. Mod. Phys. 89 (4) (2017) 045002. [arXiv:1611.09748](#), [doi:10.1103/RevModPhys.89.045002](#).
- [20] R. D. Ball, V. Bertone, S. Carrazza, L. D. Debbio, S. Forte, P. Groth-Merrild, A. Guffanti, N. P. Hartland, Z. Kassabov, J. I. Latorre, E. R. Nocera, J. Rojo, L. Rottoli, E. Slade, M. Ubiali, Parton distributions from high-precision collider data: NNPDF Collaboration, The European Physical Journal C 77 (10) (2017) 663. [arXiv:1706.00428](#), [doi:10.1140/epjc/s10052-017-5199-5](#).
- [21] R. L. Jaffe, Parton Distribution Functions for Twist Four, Nucl. Phys. B 229 (1983) 205–230. [doi:10.1016/0550-3213\(83\)90361-9](#).
- [22] X.-D. Ji, Off forward parton distributions, J. Phys. G 24 (1998) 1181–1205. [arXiv:hep-ph/9807358](#), [doi:10.1088/0954-3899/24/7/002](#).
- [23] M. V. Polyakov, C. Weiss, Skewed and double distributions in pion and nucleon, Phys. Rev. D 60 (1999) 114017. [arXiv:hep-ph/9902451](#), [doi:10.1103/PhysRevD.60.114017](#).
- [24] K. Goeke, M. V. Polyakov, M. Vanderhaeghen, Hard exclusive reactions and the structure of hadrons, Prog. Part. Nucl. Phys. 47 (2001) 401–515. [arXiv:hep-ph/0106012](#), [doi:10.1016/S0146-6410\(01\)00158-2](#).
- [25] A. V. Belitsky, A. V. Radyushkin, Unraveling hadron structure with generalized parton distributions, Phys. Rept. 418 (2005) 1–387. [arXiv:hep-ph/0504030](#), [doi:10.1016/j.physrep.2005.06.002](#).
- [26] J. Collins, New definition of TMD parton densities, Int. J. Mod. Phys. Conf. Ser. 4 (2011) 85–96. [arXiv:1107.4123](#), [doi:10.1142/S2010194511001590](#).
- [27] R. Angeles-Martinez, et al., Transverse Momentum Dependent (TMD) parton distribution functions: status and prospects, Acta Phys. Polon. B 46 (12) (2015) 2501–2534. [arXiv:1507.05267](#), [doi:10.5506/APhysPolB.46.2501](#).
- [28] M. Diehl, Introduction to GPDs and TMDs, Eur. Phys. J. A 52 (6) (2016) 149. [arXiv:1512.01328](#), [doi:10.1140/epja/i2016-16149-3](#).
- [29] A. Bacchetta, Where do we stand with a 3-D picture of the proton?, Eur. Phys. J. A 52 (6) (2016) 163. [arXiv:2107.06772](#), [doi:10.1140/epja/i2016-16163-5](#).
- [30] M. Burkardt, Impact parameter dependent parton distributions and off forward parton distributions for $\zeta \rightarrow 0$, Phys. Rev. D 62 (2000) 071503, [Erratum: Phys.Rev.D 66, 119903 (2002)]. [arXiv:hep-ph/0005108](#), [doi:10.1103/PhysRevD.62.071503](#).
- [31] M. Burkardt, Impact parameter space interpretation for generalized parton distributions, Int. J. Mod. Phys. A 18 (2003) 173–208. [arXiv:hep-ph/0207047](#), [doi:10.1142/S0217751X03012370](#).
- [32] Y. Liu, S. Xu, C. Mondal, X. Zhao, J. P. Vary, Angular momentum and generalized parton distributions for the proton with basis light-front quantization, Phys. Rev. D 105 (9) (2022) 094018. [arXiv:2202.00985](#), [doi:10.1103/PhysRevD.105.094018](#).
- [33] X.-D. Ji, Deeply virtual Compton scattering, Phys. Rev. D 55 (1997) 7114–7125. [arXiv:hep-ph/9609381](#), [doi:10.1103/PhysRevD.55.7114](#).
- [34] L. Favart, M. Guidal, T. Horn, P. Kroll, Deeply Virtual Meson Production on the nucleon, Eur. Phys. J. A 52 (6) (2016) 158. [arXiv:1511.04535](#), [doi:10.1140/epja/i2016-16158-2](#).
- [35] S. Boffi, B. Pasquini, Generalized parton distributions and the structure of the nucleon, Riv. Nuovo Cim. 30 (9) (2007) 387–448. [arXiv:0711.2625](#), [doi:10.1393/ncr/i2007-10025-7](#).
- [36] D. Boer, P. J. Mulders, Time reversal odd distribution functions in lepton production, Phys. Rev. D 57 (1998) 5780–5786. [arXiv:hep-ph/9711485](#), [doi:10.1103/PhysRevD.57.5780](#).
- [37] S. J. Brodsky, D. S. Hwang, I. Schmidt, Initial state interactions and single spin asymmetries in Drell-Yan processes, Nucl. Phys. B 642 (2002) 344–356. [arXiv:hep-ph/0206259](#), [doi:10.1016/S0550-3213\(02\)00617-X](#).
- [38] S. J. Brodsky, D. S. Hwang, I. Schmidt, Final state interactions and single spin asymmetries in semiinclusive deep inelastic scattering, Phys. Lett. B 530 (2002) 99–107. [arXiv:hep-ph/0201296](#), [doi:10.1016/S0370-2693\(02\)01320-5](#).
- [39] A. Bacchetta, G. Bozzi, M. G. Echevarria, C. Pisano, A. Prokudin, M. Radici, Azimuthal asymmetries in unpolarized sidis and drell-yan processes: A case study towards tmd factorization at subleading twist, Physics Letters B 797 (2019) 134850. [doi:10.1016/j.physletb.2019.134850](#). URL <http://dx.doi.org/10.1016/j.physletb.2019.134850>
- [40] V. Barone, A. Drago, P. G. Ratcliffe, Transverse polarisation of quarks in hadrons, Phys. Rept. 359 (2002) 1–168. [arXiv:hep-ph/0104283](#), [doi:10.1016/S0370-1573\(01\)00051-5](#).
- [41] S. M. Aybat, T. C. Rogers, TMD Parton Distribution and Fragmentation Functions with QCD Evolu-

- tion, Phys. Rev. D 83 (2011) 114042. [arXiv:1101.5057](#), [doi:10.1103/PhysRevD.83.114042](#).
- [42] R. L. Jaffe, X. Ji, Chiral-odd parton distributions and polarized Drell-Yan process, Physical Review Letters 67 (5) (1991) 552–555. [doi:10.1103/PhysRevLett.67.552](#).
- [43] R. L. Jaffe, X.-D. Ji, Chiral odd parton distributions and Drell-Yan processes, Nucl. Phys. B 375 (1992) 527–560. [doi:10.1016/0550-3213\(92\)90110-W](#).
- [44] A. V. Efremov, P. Schweitzer, The Chirally odd twist 3 distribution $e(a)(x)$, JHEP 08 (2003) 006. [arXiv:hep-ph/0212044](#), [doi:10.1088/1126-6708/2003/08/006](#).
- [45] R. Abdul Khalek, et al., Science Requirements and Detector Concepts for the Electron-Ion Collider: EIC Yellow Report, Nucl. Phys. A 1026 (2022) 122447. [arXiv:2103.05419](#), [doi:10.1016/j.nuclphysa.2022.122447](#).
- [46] S. Wandzura, F. Wilczek, Sum Rules for Spin Dependent Electroproduction: Test of Relativistic Constituent Quarks, Phys. Lett. B 72 (1977) 195–198. [doi:10.1016/0370-2693\(77\)90700-6](#).
- [47] A. Bacchetta, G. Bozzi, M. G. Echevarria, C. Pisano, A. Prokudin, M. Radici, Azimuthal asymmetries in unpolarized SIDIS and Drell-Yan processes: a case study towards TMD factorization at subleading twist, Phys. Lett. B 797 (2019) 134850. [arXiv:1906.07037](#), [doi:10.1016/j.physletb.2019.134850](#).
- [48] A. Freund, Detailed qcd analysis of twist-3 effects in deeply virtual compton scattering observables, Physical Review D 68 (9) (Nov. 2003). [doi:10.1103/physrevd.68.096006](#). URL <http://dx.doi.org/10.1103/PhysRevD.68.096006>
- [49] P. J. Mulders, R. D. Tangerman, The Complete tree level result up to order $1/Q$ for polarized deep inelastic leptoproduction, Nucl. Phys. B 461 (1996) 197–237, [Erratum: Nucl.Phys.B 484, 538–540 (1997)]. [arXiv:hep-ph/9510301](#), [doi:10.1016/0550-3213\(95\)00632-X](#).
- [50] H. Avakian, et al., Jlab experiment (2008).
- [51] H. Avakian, et al., Jlab experiment (2006).
- [52] S. Pisano, et al., Jlab experiment (2014).
- [53] R. Abdul Khalek, et al., Snowmass 2021 White Paper: Electron Ion Collider for High Energy Physics (3 2022). [arXiv:2203.13199](#).
- [54] S. Amoroso, et al., Snowmass 2021 Whitepaper: Proton Structure at the Precision Frontier, Acta Phys. Polon. B 53 (12) (2022) 12–A1. [arXiv:2203.13923](#), [doi:10.5506/APhysPolB.53.12-A1](#).
- [55] D. P. Anderle, et al., Electron-ion collider in China, Front. Phys. (Beijing) 16 (6) (2021) 64701. [arXiv:2102.09222](#), [doi:10.1007/s11467-021-1062-0](#).
- [56] D. Boer, et al., Gluons and the quark sea at high energies: Distributions, polarization, tomography (8 2011). [arXiv:1108.1713](#).
- [57] R. Jakob, P. J. Mulders, J. Rodrigues, Modeling quark distribution and fragmentation functions, Nucl. Phys. A 626 (1997) 937–965. [arXiv:hep-ph/9704335](#), [doi:10.1016/S0375-9474\(97\)00588-5](#).
- [58] Z. Lu, I. Schmidt, T-odd quark-gluon-quark correlation function in the diquark model, Phys. Lett. B 712 (2012) 451–455. [arXiv:1202.0700](#), [doi:10.1016/j.physletb.2012.05.023](#).
- [59] W. Mao, Z. Lu, Beam spin asymmetries of charged and neutral pion production in semi-inclusive DIS, Eur. Phys. J. C 73 (2013) 2557. [arXiv:1306.1004](#), [doi:10.1140/epjc/s10052-013-2557-9](#).
- [60] W. Mao, Z. Lu, B.-Q. Ma, Transverse single-spin asymmetries of pion production in semi-inclusive DIS at subleading twist, Phys. Rev. D 90 (1) (2014) 014048. [arXiv:1405.3876](#), [doi:10.1103/PhysRevD.90.014048](#).
- [61] A. I. Signal, Calculations of higher twist distribution functions in the MIT bag model, Nucl. Phys. B 497 (1997) 415–434. [arXiv:hep-ph/9610480](#), [doi:10.1016/S0550-3213\(97\)00231-9](#).
- [62] H. Avakian, A. V. Efremov, P. Schweitzer, F. Yuan, The transverse momentum dependent distribution functions in the bag model, Phys. Rev. D 81 (2010) 074035. [arXiv:1001.5467](#), [doi:10.1103/PhysRevD.81.074035](#).
- [63] C. Lorcé, B. Pasquini, P. Schweitzer, Unpolarized transverse momentum dependent parton distribution functions beyond leading twist in quark models, JHEP 01 (2015) 103. [arXiv:1411.2550](#), [doi:10.1007/JHEP01\(2015\)103](#).
- [64] P. Schweitzer, The Chirally odd twist three distribution function $e^*\alpha(x)$ in the chiral quark soliton model, Phys. Rev. D 67 (2003) 114010. [arXiv:hep-ph/0303011](#), [doi:10.1103/PhysRevD.67.114010](#).
- [65] M. Wakamatsu, Comparative analysis of the transversities and the longitudinally polarized distribution functions of the nucleon, Phys. Lett. B 653 (2007) 398–403. [arXiv:0705.2917](#), [doi:10.1016/j.physletb.2007.08.013](#).
- [66] M. Wakamatsu, Y. Ohnishi, The Nonperturbative origin of delta function singularity in the chirally odd twist three distribution function $e(x)$, Phys. Rev. D 67 (2003) 114011. [arXiv:hep-ph/0303007](#), [doi:10.1103/PhysRevD.67.114011](#).
- [67] Y. Ohnishi, M. Wakamatsu, pi N sigma term and chiral odd twist three distribution function $e(x)$ of the nucleon in the chiral quark soliton model, Phys. Rev. D 69 (2004) 114002. [arXiv:hep-ph/0312044](#), [doi:10.1103/PhysRevD.69.114002](#).
- [68] C. Cebulla, J. Ossmann, P. Schweitzer, D. Urbano, The Twist-3 parton distribution function $e^*a(x)$ in large- $N(c)$ chiral theory, Acta Phys. Polon. B 39 (2008) 609–640. [arXiv:0710.3103](#).
- [69] J. Balla, M. V. Polyakov, C. Weiss, Nucleon matrix elements of higher twist operators from the instanton vacuum, Nucl. Phys. B 510 (1998) 327–364. [arXiv:hep-ph/9707515](#), [doi:10.1016/S0550-3213\(98\)00638-5](#).
- [70] B. Dressler, M. V. Polyakov, On the twist - three contribution to $h(L)$ in the instanton vacuum, Phys. Rev. D 61 (2000) 097501. [arXiv:hep-ph/9912376](#), [doi:10.1103/PhysRevD.61.097501](#).
- [71] C. Lorcé, B. Pasquini, P. Schweitzer, Transverse pion structure beyond leading twist in constituent models, Eur. Phys. J. C 76 (7) (2016) 415. [arXiv:1605.00815](#), [doi:10.1140/epjc/s10052-016-4257-8](#).
- [72] B. Pasquini, S. Rodini, The twist-three distribution $e^q(x, k_\perp)$ in a light-front model, Phys. Lett. B 788 (2019) 414–424. [arXiv:1806.10932](#), [doi:10.1016/j.physletb.2018.11.033](#).
- [73] M. Burkardt, Y. Koike, Violation of sum rules for twist three parton distributions in QCD, Nucl. Phys. B 632 (2002) 311–329. [arXiv:hep-ph/0111343](#), [doi:10.1016/S0550-3213\(02\)00263-8](#).
- [74] R. Kundu, A. Metz, Higher twist and trans-

- verse momentum dependent parton distributions: A Light front Hamiltonian approach, *Phys. Rev. D* 65 (2002) 014009. [arXiv:hep-ph/0107073](#), [doi:10.1103/PhysRevD.65.014009](#).
- [75] A. Mukherjee, Twist Three Distribution $e(x)$: Sum Rules and Equation of Motion Relations, *Phys. Lett. B* 687 (2010) 180–183. [arXiv:0912.1446](#), [doi:10.1016/j.physletb.2010.03.023](#).
- [76] A. Accardi, A. Bacchetta, W. Melnitchouk, M. Schlegel, What can break the Wandzura-Wilczek relation?, *JHEP* 11 (2009) 093. [arXiv:0907.2942](#), [doi:10.1088/1126-6708/2009/11/093](#).
- [77] Y. Choi, A. J. Arifi, H.-M. Choi, C.-R. Ji, Kaon T-even transverse-momentum-dependent distributions and form factors in a self-consistent light-front quark model (12 2025). [arXiv:2512.21642](#).
- [78] W. de Paula, T. Frederico, G. Salmè, Unpolarized transverse-momentum dependent distribution functions of a quark in a pion with Minkowskian dynamics, *Eur. Phys. J. C* 83 (10) (2023) 985. [arXiv:2301.11599](#), [doi:10.1140/epjc/s10052-023-12119-0](#).
- [79] Z. Zhu, Z. Hu, J. Lan, C. Mondal, X. Zhao, J. P. Vary, Transverse structure of the pion beyond leading twist with basis light-front quantization, *Phys. Lett. B* 839 (2023) 137808. [arXiv:2301.12994](#), [doi:10.1016/j.physletb.2023.137808](#).
- [80] M. Cerutti, L. Rossi, S. Venturini, A. Bacchetta, V. Bertone, C. Bissolotti, M. Radici, Extraction of pion transverse momentum distributions from Drell-Yan data, *Phys. Rev. D* 107 (1) (2023) 014014. [arXiv:2210.01733](#), [doi:10.1103/PhysRevD.107.014014](#).
- [81] P. C. Barry, L. Gamberg, W. Melnitchouk, E. Moffat, D. Pitonyak, A. Prokudin, N. Sato, Tomography of pions and protons via transverse momentum dependent distributions (2 2023). [arXiv:2302.01192](#).
- [82] J. Lan, J. Chen, Z. Zhu, C. Mondal, X. Zhao, J. P. Vary, Strange mesons with one dynamical gluon: A light-front approach, *Phys. Lett. B* 868 (2025) 139654. [arXiv:2501.03476](#), [doi:10.1016/j.physletb.2025.139654](#).
- [83] M. Woods, K. Nishikawa, J. R. Patterson, Y. W. Wah, B. Winstein, R. Winston, H. Yamamoto, E. C. Swallow, G. J. Bock, R. Coleman, Y. B. Hsiung, K. Stanfield, R. Stefanski, T. Yamanaka, G. D. Gollin, G. L. Grazer, J. K. Okamitsu, P. Jarry, R. Daudin, P. Debu, B. Peyaud, R. Turlay, **First result on a new measurement of ϵ'/ϵ in the neutral-kaon system**, *Phys. Rev. Lett.* 60 (1988) 1695–1698. [doi:10.1103/PhysRevLett.60.1695](#).
URL <https://link.aps.org/doi/10.1103/PhysRevLett.60.1695>
- [84] G. Barr, P. Buchholz, R. Carosi, D. Coward, D. Cundy, N. Doble, L. Gatignon, V. Gibson, P. Grafström, R. Hagelberg, J. van der Lans, H. Nelson, H. Wahl, K. Peach, H. Blümer, R. Heinz, K. Kleinknecht, P. Mayer, B. Panzer, B. Renk, H. Rohrer, H. Sander, A. Wagner, E. Augé, D. Fournier, P. Heusse, L. Iconomidou-Fayard, I. Harrus, O. Perdereau, A. Schaffer, L. Serin, L. Bertanza, A. Bigi, P. Calafiura, M. Calvetti, M. Carrozza, R. Casali, C. Cerri, R. Fantechi, I. Mannelli, V. Marzulli, A. Nappi, G. Pierazzini, M. Holder, A. Kreutz, G. Quast, M. Rost, R. Werthenbach, G. Zech, **A new measurement of direct cp violation in the neutral kaon system**, *Physics Letters B* 317 (1) (1993) 233–242. [doi:https://doi.org/10.1016/0370-2693\(93\)91599-I](#).
URL <https://www.sciencedirect.com/science/article/pii/037026939391599I>
- [85] R. Adler, et al., Measurement of the CP violation parameter η_{+-} using tagged K_0 and anti- K_0 , *Phys. Lett. B* 363 (1995) 243–248. [doi:10.1016/0370-2693\(95\)01295-0](#).
- [86] J. P. Vary, H. Honkanen, J. Li, P. Maris, S. J. Brodsky, A. Harindranath, G. F. de Teramond, P. Sternberg, E. G. Ng, C. Yang, Hamiltonian light-front field theory in a basis function approach, *Phys. Rev. C* 81 (2010) 035205. [arXiv:0905.1411](#), [doi:10.1103/PhysRevC.81.035205](#).
- [87] X. Zhao, H. Honkanen, P. Maris, J. P. Vary, S. J. Brodsky, Electron g-2 in Light-Front Quantization, *Phys. Lett. B* 737 (2014) 65–69. [arXiv:1402.4195](#), [doi:10.1016/j.physletb.2014.08.020](#).
- [88] P. Wiecki, Y. Li, X. Zhao, P. Maris, J. P. Vary, Basis Light-Front Quantization Approach to Positronium, *Phys. Rev. D* 91 (10) (2015) 105009. [arXiv:1404.6234](#), [doi:10.1103/PhysRevD.91.105009](#).
- [89] Y. Li, P. Maris, X. Zhao, J. P. Vary, Heavy Quarkonium in a Holographic Basis, *Phys. Lett. B* 758 (2016) 118–124. [arXiv:1509.07212](#), [doi:10.1016/j.physletb.2016.04.065](#).
- [90] S. Jia, J. P. Vary, Basis light front quantization for the charged light mesons with color singlet Nambu–Jona-Lasinio interactions, *Phys. Rev. C* 99 (3) (2019) 035206. [arXiv:1811.08512](#), [doi:10.1103/PhysRevC.99.035206](#).
- [91] W. Qian, S. Jia, Y. Li, J. P. Vary, Light mesons within the basis light-front quantization framework, *Phys. Rev. C* 102 (5) (2020) 055207. [arXiv:2005.13806](#), [doi:10.1103/PhysRevC.102.055207](#).
- [92] S. Tang, Y. Li, P. Maris, J. P. Vary, Heavy-light mesons on the light front, *Eur. Phys. J. C* 80 (6) (2020) 522. [arXiv:1912.02088](#), [doi:10.1140/epjc/s10052-020-8081-9](#).
- [93] C. Mondal, S. Xu, J. Lan, X. Zhao, Y. Li, D. Chakrabarti, J. P. Vary, Proton structure from a light-front Hamiltonian, *Phys. Rev. D* 102 (1) (2020) 016008. [arXiv:1911.10913](#), [doi:10.1103/PhysRevD.102.016008](#).
- [94] S. Xu, C. Mondal, J. Lan, X. Zhao, Y. Li, J. P. Vary, Nucleon structure from basis light-front quantization, *Phys. Rev. D* 104 (9) (2021) 094036. [arXiv:2108.03909](#), [doi:10.1103/PhysRevD.104.094036](#).
- [95] S. Nair, C. Mondal, X. Zhao, A. Mukherjee, J. P. Vary, Basis light-front quantization approach to photon, *Phys. Lett. B* 827 (2022) 137005. [arXiv:2201.12770](#), [doi:10.1016/j.physletb.2022.137005](#).
- [96] J. Lan, K. Fu, C. Mondal, X. Zhao, J. P. Vary, Light mesons with one dynamical gluon on the light front, *Phys. Lett. B* 825 (2022) 136890. [arXiv:2106.04954](#), [doi:10.1016/j.physletb.2022.136890](#).
- [97] L. Adhikari, C. Mondal, S. Nair, S. Xu, S. Jia, X. Zhao, J. P. Vary, Generalized parton distributions and spin structures of light mesons from a light-front Hamiltonian approach, *Phys. Rev. D* 104 (11) (2021) 114019. [arXiv:2110.05048](#), [doi:10.1103/PhysRevD.104.114019](#).
- [98] C. Mondal, S. Nair, S. Jia, X. Zhao, J. P. Vary, Pion to photon transition form factors with basis light-front quantization, *Phys. Rev. D* 104 (9) (2021)

094034. [arXiv:2109.02279](#), [doi:10.1103/PhysRevD.104.094034](#).
- [99] Z. Hu, S. Xu, C. Mondal, X. Zhao, J. P. Vary, Transverse structure of electron in momentum space in basis light-front quantization, *Phys. Rev. D* 103 (3) (2021) 036005. [arXiv:2010.12498](#), [doi:10.1103/PhysRevD.103.036005](#).
- [100] J. Lan, C. Mondal, M. Li, Y. Li, S. Tang, X. Zhao, J. P. Vary, Parton Distribution Functions of Heavy Mesons on the Light Front, *Phys. Rev. D* 102 (1) (2020) 014020. [arXiv:1911.11676](#), [doi:10.1103/PhysRevD.102.014020](#).
- [101] J. Lan, C. Mondal, S. Jia, X. Zhao, J. P. Vary, Pion and kaon parton distribution functions from basis light front quantization and QCD evolution, *Phys. Rev. D* 101 (3) (2020) 034024. [arXiv:1907.01509](#), [doi:10.1103/PhysRevD.101.034024](#).
- [102] J. Lan, C. Mondal, S. Jia, X. Zhao, J. P. Vary, Parton Distribution Functions from a Light Front Hamiltonian and QCD Evolution for Light Mesons, *Phys. Rev. Lett.* 122 (17) (2019) 172001. [arXiv:1901.11430](#), [doi:10.1103/PhysRevLett.122.172001](#).
- [103] S. Xu, C. Mondal, X. Zhao, Y. Li, J. P. Vary, Nucleon spin decomposition with one dynamical gluon (9 2022). [arXiv:2209.08584](#).
- [104] T. Peng, Z. Zhu, S. Xu, X. Liu, C. Mondal, X. Zhao, J. P. Vary, Basis light-front quantization approach to Λ and Λ_c and their isospin triplet baryons, *Phys. Rev. D* 106 (11) (2022) 114040. [arXiv:2208.00355](#), [doi:10.1103/PhysRevD.106.114040](#).
- [105] Z. Hu, S. Xu, C. Mondal, X. Zhao, J. P. Vary, Transverse momentum structure of proton within the basis light-front quantization framework, *Phys. Lett. B* 833 (2022) 137360. [arXiv:2205.04714](#), [doi:10.1016/j.physletb.2022.137360](#).
- [106] Z. Zhang, Z. Hu, S. Xu, C. Mondal, X. Zhao, J. P. Vary, Twist-3 generalized parton distribution for the proton from basis light-front quantization, *Phys. Rev. D* 109 (3) (2024) 034031. [arXiv:2312.00667](#), [doi:10.1103/PhysRevD.109.034031](#).
- [107] Y. Liu, S. Xu, C. Mondal, Z. Hu, X. Zhao, J. P. Vary, Skewed generalized parton distributions of proton from basis light-front quantization, *Phys. Lett. B* 855 (2024) 138809. [arXiv:2403.05922](#), [doi:10.1016/j.physletb.2024.138809](#).
- [108] H. Yu, Z. Hu, S. Xu, C. Mondal, X. Zhao, J. P. Vary, Transverse-momentum-dependent gluon distributions of proton within basis light-front quantization, *Phys. Lett. B* 855 (2024) 138831. [arXiv:2403.06125](#), [doi:10.1016/j.physletb.2024.138831](#).
- [109] J. C. Collins, D. E. Soper, Back-To-Back Jets: Fourier Transform from B to K-Transverse, *Nucl. Phys. B* 197 (1982) 446–476. [doi:10.1016/0550-3213\(82\)90453-9](#).
- [110] S. Catani, D. de Florian, M. Grazzini, Universality of nonleading logarithmic contributions in transverse momentum distributions, *Nucl. Phys. B* 596 (2001) 299–312. [arXiv:hep-ph/0008184](#), [doi:10.1016/S0550-3213\(00\)00617-9](#).
- [111] G. Bozzi, S. Catani, D. de Florian, M. Grazzini, Transverse-momentum resummation and the spectrum of the Higgs boson at the LHC, *Nucl. Phys. B* 737 (2006) 73–120. [arXiv:hep-ph/0508068](#), [doi:10.1016/j.nuclphysb.2005.12.022](#).
- [112] G. Bozzi, S. Catani, G. Ferrera, D. de Florian, M. Grazzini, Transverse-momentum resummation: A Perturbative study of Z production at the Tevatron, *Nucl. Phys. B* 815 (2009) 174–197. [arXiv:0812.2862](#), [doi:10.1016/j.nuclphysb.2009.02.014](#).
- [113] S. J. Brodsky, H.-C. Pauli, S. S. Pinsky, Quantum chromodynamics and other field theories on the light cone, *Physics Reports* 301 (4-6) (1998) 299–486. [arXiv:hep-ph/9705477](#), [doi:10.1016/S0370-1573\(97\)00089-6](#).
- [114] W. Qian, S. Jia, Y. Li, J. P. Vary, Light mesons within the basis light-front quantization framework, *Physical Review C* 102 (5) (2020) 1–12. [arXiv:2005.13806](#), [doi:10.1103/PhysRevC.102.055207](#).
- [115] J. Lan, J. Chen, Z. Zhu, C. Mondal, X. Zhao, J. P. Vary, **Strange mesons with one dynamical gluon: A light-front approach** (2025). [arXiv:2501.03476](#). URL <https://arxiv.org/abs/2501.03476>
- [116] P. C. Barry, C.-R. Ji, W. Melnitchouk, N. Sato, F. Steffens, First simultaneous global QCD analysis of kaon and pion parton distributions with lattice QCD constraints (10 2025). [arXiv:2510.11979](#).
- [117] J. Lan, K. Fu, C. Mondal, X. Zhao, J. P. Vary, Light mesons with one dynamical gluon within basis light-front quantization, in: 19th International Conference on Hadron Spectroscopy and Structure, 2022. [arXiv:2201.05987](#).
- [118] S. J. Brodsky, H.-C. Pauli, S. S. Pinsky, **Quantum chromodynamics and other field theories on the light cone**, *Physics Reports* 301 (4–6) (1998) 299–486. [doi:10.1016/s0370-1573\(97\)00089-6](#). URL [http://dx.doi.org/10.1016/S0370-1573\(97\)00089-6](http://dx.doi.org/10.1016/S0370-1573(97)00089-6)
- [119] M. Burkardt, Dynamical vertex mass generation and chiral symmetry breaking on the light front, *Phys. Rev. D* 58 (1998) 096015. [arXiv:hep-th/9805088](#), [doi:10.1103/PhysRevD.58.096015](#).
- [120] S. D. Glazek, R. J. Perry, Special example of relativistic Hamiltonian field theory, *Phys. Rev. D* 45 (1992) 3740–3754. [doi:10.1103/PhysRevD.45.3740](#).
- [121] S. J. Brodsky, G. F. de Teramond, H. G. Dosch, J. Erlich, Light-Front Holographic QCD and Emerging Confinement, *Phys. Rept.* 584 (2015) 1–105. [arXiv:1407.8131](#), [doi:10.1016/j.physrep.2015.05.001](#).
- [122] J. P. Vary, H. Honkanen, J. Li, P. Maris, S. J. Brodsky, A. Harindranath, G. F. de Teramond, P. Sternberg, E. G. Ng, C. Yang, **Hamiltonian light-front field theory in a basis function approach**, *Physical Review C* 81 (3) (Mar. 2010). [doi:10.1103/physrevc.81.035205](#). URL <http://dx.doi.org/10.1103/PhysRevC.81.035205>
- [123] X. Zhao, A. Ilderton, P. Maris, J. P. Vary, Scattering in Time-Dependent Basis Light-Front Quantization, *Phys. Rev. D* 88 (2013) 065014. [arXiv:1303.3273](#), [doi:10.1103/PhysRevD.88.065014](#).
- [124] S. Kaur, J. Wu, Z. Hu, J. Lan, C. Mondal, X. Zhao, J. P. Vary, Quark and gluon distributions in ρ -meson from basis light-front quantization, *Phys. Lett. B* 851 (2024) 138563. [arXiv:2401.03480](#), [doi:10.1016/j.physletb.2024.138563](#).
- [125] S. Meißner, K. Goeke, A. Metz, M. Schlegel, **Generalized parton correlation functions for a spin-0 hadron**, *Journal of High Energy Physics* 2008 (08) (2008) 038–038. [doi:10.1088/1126-6708/2008/08/038](#). URL <http://dx.doi.org/10.1088/1126-6708/2008/08/038>

- [//link.springer.com/10.1007/JHEP06\(2017\)081](https://link.springer.com/10.1007/JHEP06(2017)081)
- [152] M. Anselmino, M. Boglione, J. O. Gonzalez H., S. Melis, A. Prokudin, Unpolarised transverse momentum dependent distribution and fragmentation functions from SIDIS multiplicities, *Journal of High Energy Physics* 2014 (4) (2014). doi:10.1007/JHEP04(2014)005.
- [153] S. Bhattacharya, Z.-B. Kang, A. Metz, G. Penn, D. Pitonyak, **First global QCD analysis of the TMD g_{1T} from semi-inclusive DIS data**, Not published yet (oct 2021). arXiv:2110.10253.
URL <http://arxiv.org/abs/2110.10253>
- [154] M. Anselmino, M. Boglione, U. D'Alesio, J. O. Hernandez, S. Melis, F. Murgia, A. Prokudin, Collins functions for pions from SIDIS and new e^+e^- data: A first glance at their transverse momentum dependence, *Physical Review D - Particles, Fields, Gravitation and Cosmology* 92 (11) (2015). doi:10.1103/PhysRevD.92.114023.
- [155] U. D'Alesio, C. Flore, A. Prokudin, **Role of the Soffer bound in determination of transversity and the tensor charge**, *Physics Letters, Section B: Nuclear, Elementary Particle and High-Energy Physics* 803 (2020) 135347. doi:10.1016/j.physletb.2020.135347.
URL <https://doi.org/10.1016/j.physletb.2020.135347>
- [156] J. Cammarota, L. P. Gamberg, Z. B. Kang, J. A. Miller, D. Pitonyak, A. Prokudin, T. C. Rogers, N. Sato, **Origin of single transverse-spin asymmetries in high-energy collisions**, *Physical Review D* 102 (5) (2020) 54002. arXiv:2002.08384, doi:10.1103/PhysRevD.102.054002.
URL <https://doi.org/10.1103/PhysRevD.102.054002>
- [157] C. Lefky, A. Prokudin, Extraction of the distribution function h_{1T} from experimental data, *Physical Review D - Particles, Fields, Gravitation and Cosmology* 91 (3) (2015) 1–14. arXiv:1411.0580, doi:10.1103/PhysRevD.91.034010.
- [158] Z. Zhu, S. Xu, J. Wu, H. Yu, Z. Hu, J. Lan, C. Mondal, X. Zhao, J. P. Vary, Transverse structure of the proton beyond leading twist: A light-front Hamiltonian approach, *Phys. Lett. B* 855 (2024) 138829. arXiv:2404.13720, doi:10.1016/j.physletb.2024.138829.
- [159] K. Golec-Biernat, Partonic Entropy of the Proton from DGLAP Evolution (12 2025). arXiv:2512.23102.
- [160] C. Hampson, M. Guzzi, DGLAP evolution at N^3 LO with the **Candia** algorithm (12 2025). arXiv:2512.22667.
- [161] J. M. M. Chávez, V. Bertone, F. De Soto Borrero, M. Defurne, C. Mezrag, H. Moutarde, J. Rodríguez-Quintero, J. Segovia, Accessing the Pion 3D Structure at US and China Electron-Ion Colliders, *Phys. Rev. Lett.* 128 (20) (2022) 202501. arXiv:2110.09462, doi:10.1103/PhysRevLett.128.202501.